(b) Structure Determination. The 3860 raw intensity data were converted to structure factor amplitudes and their esd's by correction for scan speed, background, and Lorentz and polarization effects. An empirical absorption correction based on azimuthal scan data (T_{max} = 1.000, T_{min} = 0.959) was applied. Inspection of the systematic absences indicated space group $P2_1/n$. Removal of systematically absent and redundant data left 3771 unique data in the final data set.

The structure was solved by Patterson methods and refined via standard least-squares and Fourier techniques. The final residuals for 141 variables refined against the 3230 data for which $F_2 > 3\sigma(F^2)$ were R = 5.4%, R_w = 8.4%, and GOF = 3.83. The R value for all 2890 data was 6.3%.

The quantity minimized by the least-squares program was $\sum w(|F_o| - |F_c|)^2$, where w is the weight of a given observation. The p factor, used to reduce the weight of intense reflections, was set to 0.03 throughout the refinement. The analytical forms of the scattering factor tables for the neutral atoms were used and all scattering factors were corrected for both the real and imaginary components of anomalous dispersion.

The positional and thermal parameters of the non-hydrogen atoms are provided as supplementary material, as well as a listing of the values of F_o and F_c.

Acknowledgment. We greatly appreciate support for this work from the National Institutes of Health (Grant GM-25459). Crystal structures were performed by Dr. Frederick J. Hollander at the University of California, Berkeley (CHEXRAY) facility.

Supplementary Material Available: Tables of positional parameters, anisotropic thermal parameters, and anisotropic displacements for compounds 7 and 10, as well as the positions and thermal parameters of hydrogen atoms (6 pages); structure factor tables for 7 and 10 (42 pages). This material is provided with the archival edition of the journal, available in many libraries; alternatively, ordering information is given on any current masthead page.

Structure and Reactions of Oxametallacyclobutanes and Oxametallacyclobutenes of Ruthenium

John F. Hartwig, Robert G. Bergman,* and Richard A. Andersen*

Department of Chemistry, University of California, Berkeley, California 94720

Received March 26, 1991

Structure and reactivity studies are reported with the ruthenium metallacycles prepared as described in the previous paper. A C–C cleavage reaction by an apparent β-Me elimination pathway at 45 °C is reported for the PMe_3-substituted oxametallacyclobutane complex $(PMe_3)_4Ru(OC(Me)(Ph)CH_2)$ (1), while the analogous DMPE-substituted metallacyclobutane $(DMPE)_2Ru(OC(Me)(Ph)CH_2)$ (2) is stable at 140 °C. Similarly, compound 1 undergoes insertion of CO into the metal–carbon bond, while 2 is inert toward this substrate. Addition of protic acids and electrophiles leads to rapid extrusion of α-methylstyrene with both metallacycles. X-ray structural analysis of the acetone dianion complex $(PMe_3)_4Ru((CH_2)_2CO)$ (17) was performed and displays a dihedral angle of 46 °C in the metallacycle. In contrast, the 4,4-dimethyl-2-butanone dianion complex $(PMe_3)_4Ru(CH_2C(CHCMe_3)O)$ (15) contains a flat metallacycle that is bound through the CH_2 group and the oxygen atom. Reactivity studies with 15 showed that, unlike compounds 1 and 2, the organic portion remained intact upon addition of protic acids. The addition of 4,4-dimethyl-2-butanone led to a second C–C cleavage reaction, forming the di-*tert*-butylacetylacetonate complex $(PMe_3)_3Ru(Me)(CH(COCH_2CMe_3)_2)$ (19). Reactivity studies with 17 showed reversible formation of the isolable oxatrimethylenemethane complex 18, which was isolated and structurally characterized. Addition of acetone to 17 led to formation of mesityl oxide dianion complex $(PMe_3)_4Ru(OC(Me)CHC(Me)CH)$ (19); mesityl oxide is presumably formed by aldol condensation at the metal center. Reactivity studies of the oxametallacyclobutene complex $(PMe_3)_4Ru(OC(CMe_3)CH)$ showed formation of free ketone upon addition of protic acids and insertion into the metal–oxygen bond upon addition of CO_2. The metallacycle was converted to the silyl enol ether upon addition of trimethylsilane and to the free ketone following addition of H_2.

Introduction

Oxametallacyclobutanes have been invoked as intermediates in several reactions that have found widespread utility. For example, processes such as carbonyl methylenation reactions mediated by transition-metal complexes and asymmetric epoxidation of allylic alcohols with titanium catalysts are believed to involve oxametallacyclobutane intermediates.[1] In addition, the intermediacy of oxametallacycles in the epoxidation of olefins by cytochrome P-450 catalysts has been a controversial topic,[1] and the ability to prepare such metallacycles may help to understand these oxidation processes more fully. Several other reactions of potential utility, such as rhodium-catalyzed synthesis of β-lactams from aziridines[2] and formation of a metallacyclic carbonate of platinum from epoxide and CO_2,[3] are also believed to proceed by way of oxa- and azametallacyclobutanes.

These results demonstrate that even isolable oxametallacyclobutanes should behave as reactive species. In

(1) For discussions of oxametallacyclobutanes as intermediates in titanium-mediated carbonyl methylenation reactions, see: (a) Brown-Wensley, K. A.; Buchwald, S. L.; Cannizzo, L.; Clawson, L.; Ho, S.; Meinhardt, D.; Stille, J. R.; Straus, D.; Grubbs, R. H. *Pure Appl. Chem.* **1983**, *55*, 1733. As intermediates in asymmetric epoxidations, see: (b) Sharpless, K. B.; Teranishi, A. Y.; Backvall, J.-E. *J. Am. Chem. Soc.* **1977**, *99*, 3120. (c) Rappe, A. K.; Goddard, W. A. *J. Am. Chem. Soc.* **1982**, *104*, 3287. With P-450 models, see: (d) Collman, J. P.; Brauman, J. I.; Meunier, B.; Raybuck, S. A.; Kodadek, T. *Proc. Natl. Acad. Sci. U.S.A.* **1984**, *81*, 3245. (e) Walba, D. M.; DePuy, C. H.; Grabowski, J. J.; Bierbaum, V. M. *Organometallics* **1984**, *3*, 498. (f) Collman, J. P.; Kodadek, T.; Raybuck, S. A.; Brauman, J. I.; Papazian, L. M. *J. Am. Chem. Soc.* **1985**, *107*, 4343. (g) Collman, J. P.; Brauman, J. I.; Meunier, B.; Hayashi, T.; Kodadek, T.; Raybuck, S. A. *J. Am. Chem. Soc.* **1985**, *107*, 2000. (h) Mock, W. L.; Bieniarz, C. *Organometallics* **1985**, *4*, 1917. (i) Groves, J. T.; Avaria-Nesser, G. E.; Fish, K. M.; Imachi, M.; Kuczkowski, R. L. *J. Am. Chem. Soc.* **1986**, *108*, 3837. (j) Girardet, M.; Meunier, B. *Tetrahedron Lett.* **1977**, 2955. (k) For a general review, see: Jorgensen, J. A.; Schiott, B. *Chem. Rev.* **1990**, *90*, 1483.

0276-7333/91/2310-3344$02.50/0 © 1991 American Chemical Society

fact, only a few examples of stable oxametallacyclobutanes are known. Late-transition-metal examples include the preparation and reactivity of iridaaza- and iridoxacylobutane complexes reported recently from our laboratories,[4] the generation of an oxametallacyclobutane of iridium by reaction of a coordinated olefin with molecular oxygen,[5] the formation of an analogous platinum complex from tetracyanooxirane (2,2,3,3-tetracyanooxacyclopropane),[6] and the recent structural characterization of a rhodium oxametallacyclobutane.[7] Early-transition-metal oxametallacyclobutanes[8] include titanium and tantalum examples. An oxametallacyclobutane of platinum containing an oxygen atom in the β-position has also been reported.[9]

Even more rare are the analogous complexes containing a C=C bond, the oxametallacyclobutenes. The only isolated examples known so far were prepared by Vaughn and Hillhouse, by the addition of N_2O to zirconocene acetylene and benzyne complexes;[10] the same complex was reported from our laboratories to form from addition of diphenylacetylene to an oxozirconocene species.[11]

Both oxametallacyclobutane and -butene complexes provide the opportunity to compare the reactivities of the metal–heteroatom and metal–carbon bonds. Metathesis with early-metal complexes forms alkene or alkyne and metal–oxo products,[1a] while the iridaoxacyclobutane complex reported from our laboratory forms ketone and metal–carbene upon photolysis.[4] In addition, insertion reactions occur with the late transition metal–heteroatom bonds in both iridium and platinum oxametallacyclobutanes, consistent with the expected reactivity based on the mismatch of a soft metal center and a hard alkoxide or amide substituent.[12]

We have recently reported the unexpected reaction of CO and CO_2 with the metal–carbon bond of a ruthenium oxametallacycle formed by orthometalation of a *p*-cresolate substituent.[13] We have also investigated the reactivities of oxametallacyclobutane and oxametallacyclobutane complexes with the goal of understanding the factors that control the selectivities of these compounds in metathesis, insertion, and epoxide-forming reactions. Several unusual reactivity patterns have been observed, including C–C bond cleavage by an apparent β-methyl elimination process, rapid C–O bond cleavage to extrude alkene upon addition of protic acids and electrophiles, and insertions into the ruthenium–oxygen and ruthenium–carbon bonds.

Scheme I

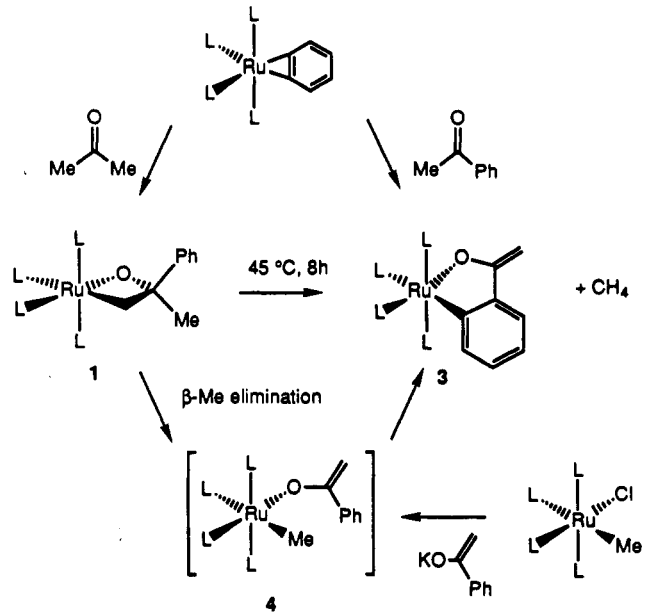

We reported preliminary reactivity with two of the metallacycles[14a,b] and subsequently set out to rationalize the initially observed reactivity patterns by synthesizing compounds with different connectivity in the ring and with different dative ligands. In this paper we report the results of these reactivity studies. Metallacycles used in this study were prepared from ruthenium enolate complexes, in most cases using methodology described in the preceding paper in this issue.[14c]

Results

Most of the results described here focus on the oxaruthenacylobutane complex $(PMe_3)_4Ru(OC(Me)(Ph)CH_2)$ (1), containing methyl and phenyl groups in the β-position of the ring. As described in the previous paper,[14c] rapid phosphine dissociation at room temperature precluded isolation of this complex in pure form. Therefore, complex 1 was characterized by solution spectroscopy. The most informative spectroscopic data included an ABCD pattern in the $^{31}P\{^1H\}$ NMR spectrum, the metal-bound CH_2 resonance in the $^{13}C\{^1H\}$ NMR spectrum, and the resonances for a terminal aryl group not bound to the ruthenium. Reactions with 1 were performed in situ following generation of the metallacycle by addition of the potassium enolate of acetone to $(PMe_3)_4Ru(Ph)(Cl)$ in hydrocarbon solutions. The DMPE analogue of 1, $(DMPE)_2Ru(OC(Me)(Ph)CH_2)$ (2), was stable enough to isolate as described in the previous paper and crystalline samples of it were used for reactivity studies.

Reactions of $(PMe_3)_4Ru(OC(Me)(Ph)CH_2)$ (1). Scheme I summarizes the thermal chemistry of compound 1. Warming a solution containing 1 of roughly 80–90% purity at 45 °C for 8 h led to formation of methane and the cyclic enolate 3 in 51% yield by ^1H NMR spectroscopy (Cp_2Fe internal standard) and in 22% isolated yield. This complex was first isolated as the product of addition of acetone to the ruthenium benzyne complex $(PMe_3)_4Ru(\eta^2\text{-}C_6H_4)$,[15] a transformation that forms one carbon–carbon

(2) (a) Alper, H.; Urso, F.; Smith, D. J. H. *J. Am. Chem. Soc.* **1983**, *105*, 6737. (b) Calet, S.; Urso, F.; Alper, H. *J. Am. Chem. Soc.* **1989**, *111*, 931.
(3) Aye, K.-T.; Ferguson, G.; Lough, A. T.; Puddephatt, R. J. *Angew. Chem., Int. Ed. Engl.* **1989**, *28*, 767.
(4) Klein, D. P.; Hayes, J. C.; Bergman, R. G. *J. Am. Chem. Soc.* **1988**, *110*, 3704.
(5) Day, V. W.; Klemperer, W. G.; Lockledge, S. P.; Main, D. J. *J. Am. Chem. Soc.* **1990**, *112*, 2031.
(6) (a) Scholdder, T.; Ibers, J. A.; Lenarda, M.; Graziani, M. *J. Am. Chem. Soc.* **1974**, *96*, 6893. (b) Lenarda, M.; Ros, R.; Traverso, O.; Pitts, W. D.; Baddley, W. H.; Graziani, M. *Inorg. Chem.* **1977**, *16*, 3178.
(7) Zlota, A. A.; Frolow, F.; Milstein, D. *J. Am. Chem. Soc.* **1990**, *112*, 6411.
(8) (a) Ho, S. C.; Hentges, S.; Grubbs, R. H. *Organometallics* **1988**, *7*, 780. (b) Bercaw, J. E., personal communication. (c) A report of molybdenum and tungsten examples appeared after submission of this paper: Bazan, G. C.; Schrock, R. R.; O'Regan, M. B. *Organometallics* **1991**, *10*, 1062.
(9) Hoover, J. F.; Stryker, J. M. *J. Am. Chem. Soc.* **1989**, *111*, 6466.
(10) (a) Vaughan, G. A.; Hillhouse, G. L.; Lum, R. T.; Buchwald, S. L.; Rheingold *J. Am. Chem. Soc.* **1988**, *110*, 7215. (b) Vaughan, G. A.; Sofield, C. D.; Hillhouse, G. L. *J. Am. Chem. Soc.* **1989**, *111*, 5491. (c) Vaughan, G. A.; Hillhouse, G. L.; Rheingold, A. L. *J. Am. Chem. Soc.* **1990**, *112*, 7994.
(11) Carney, M. J.; Walsh, P. J.; Bergman, R. G. *J. Am. Chem. Soc.* **1990**, *112*, 6426.
(12) Bryndza, H. E.; Tam, W. *Chem. Rev.* **1988**, *88*, 1163.
(13) Hartwig, J. F.; Andersen, R. A.; Bergman, R. G. *J. Am. Chem. Soc.*, in press.
(14) (a) Hartwig, J. F.; Bergman, R. G.; Andersen, R. A. *J. Am. Chem. Soc.* **1990**, *112*, 3234. (b) Hartwig, J. F.; Bergman, R. G.; Andersen, R. A. *J. Am. Chem. Soc.* **1990**, *112*, 5670. (c) Hartwig, J. F.; Andersen, R. A.; Bergman, R. G. *Organometallics*, preceding paper in this issue.
(15) Hartwig, J. F.; Bergman, R. G.; Andersen, R. A. *J. Am. Chem. Soc.* **1989**, *111*, 2717; **1991**, *113*, 3404.

Scheme II

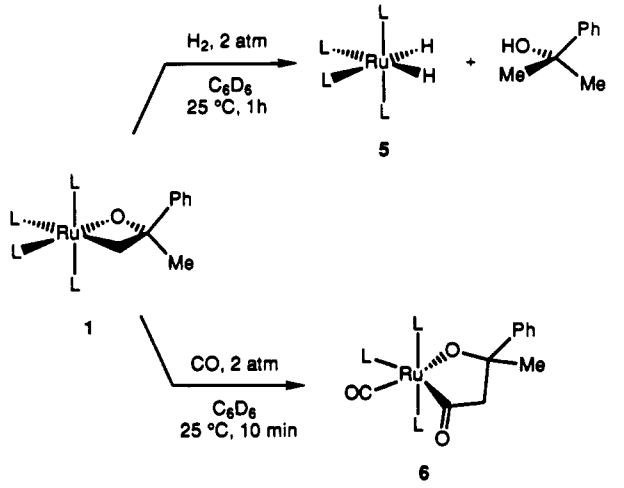

Scheme III

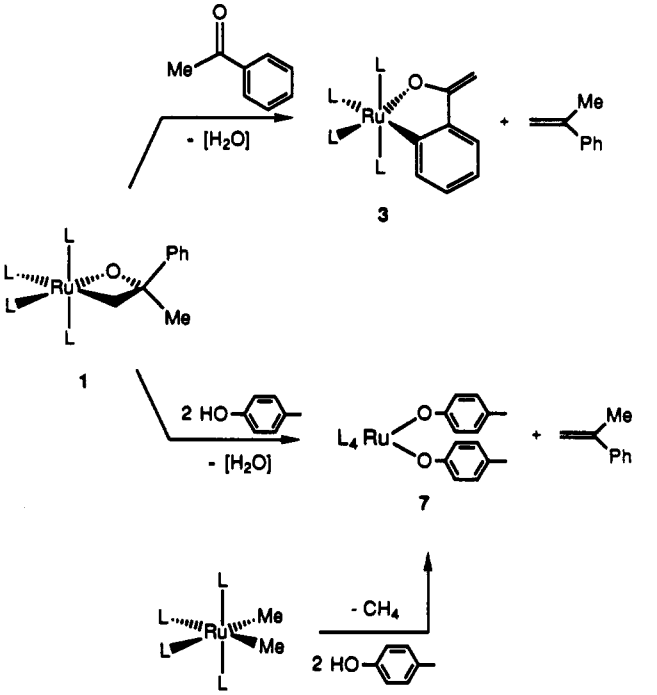

bond and cleaves another.[16] This reaction occurs by way of compound 1 as described in the previous paper; it is also conveniently formed by addition of acetophenone to the ruthenium benzyne complex $(PMe_3)_4Ru(\eta^2\text{-}C_6H_4)$.[15,17] We believe an intermediate in the thermolysis of 1 may be the methyl enolate complex $(PMe_3)_4Ru(Me)(OC(CH_2)Ph)$ (4), resulting from β-methyl elimination. In order to determine if such an intermediate forms methane and 3, 4 was generated independently by treating the methyl chloride complex $(PMe_3)_4Ru(Me)(Cl)$[18] with the potassium enolate of acetophenone. This procedure led to the formation of methane and 2 in 97% yield by ^1H NMR spectroscopy, although orthometalation was faster than substitution, precluding direct observation of 4.

Scheme II displays the reactions of 1 with hydrogen and CO. Addition of H_2 (2 atm) to a C_6D_6 solution of 1 cleanly formed the tertiary alcohol $HOCMe_2Ph$ (85% by ^1H NMR spectroscopy) and the dihydride *cis*-$(PMe_3)_4Ru(H)_2$ (5)[18,19] (88%). The ^1H NMR spectroscopic identification of the alcohol was confirmed by matching the GC retention time to that of an authentic sample.

Addition of CO (2 atm) to a solution of 1 at room temperature formed compound 6 in 51% isolated yield, the product of CO substitution at the metal center and CO insertion into the metal–carbon bond. This complex was characterized by solution NMR spectroscopy, solid-state infrared spectroscopy, and microanalysis. The infrared absorption for coordinated CO was observed at 1907 cm^{-1} and for the inserted CO at 1614 cm^{-1}. The $^{13}C\{^1H\}$ NMR spectrum displayed a resonance at 268.3 for the inserted CO and one at 201.4 for the coordinated carbonyl. The CH_2 resonance of 6 was observed as a doublet at δ 74.7, indicating that it was located in the position α to a carbonyl group and that it was no longer bound to the metal center. The CH_2 resonances for starting complex 1 was observed at much higher field (δ 0.99) and showed coupling to four phosphines. The geometry of 6 was deduced from the $^{31}P\{^1H\}$ NMR spectrum and the splitting pattern of the $^{13}C\{^1H\}$ NMR resonance corresponding to the inserted CO. The $^{31}P\{^1H\}$ NMR spectrum displayed an ABC pattern, with a large trans coupling constant of 321.1 Hz. In addition, the $^{13}C\{^1H\}$ resonance for the inserted CO showed a 100.1-Hz coupling constant, indicating that it is located trans to a phosphine ligand and that the coordinated CO, a strong π-acceptor, is located trans to the potentially π-donating oxygen of the metallacycle.

Addition of protic acids to 1 led to the extrusion of α-methylstyrene, as shown in Scheme III. The room temperature addition of *p*-cresol to a solution of 1 led to formation of α-methylstyrene in 86% yield by ^1H NMR spectroscopy and bis(cresolate) complex *cis*-$(PMe_3)_4Ru(OC_6H_4\text{-}p\text{-}Me)_2$ (7) in 74% yield. In order to maintain the proper stoichiometry, water must also be formed by this reaction, although it was not detected. Compound 7 was independently synthesized in 57% isolated yield by the addition of *p*-cresol to the dimethyl complex $(PMe_3)_4Ru(Me)_2$ during the course of a separate study.[20] Even addition of the weak acid acetophenone, followed by warming to 45 °C, led to extrusion of α-methylstyrene (58%) and formation of the cyclic enolate 3 in 61% yield by ^1H NMR spectroscopy. Presumably water was also a byproduct of this reaction.

Addition of carbon electrophiles also led to the extrusion of α-methylstyrene, as shown in Scheme IV. Addition of carbon dioxide to a solution of 1 led to formation of α-methylstyrene in 84% yield and the ruthenium carbonate $(PMe_3)_4Ru(CO_3)$ (8) in 83% yield by ^1H NMR spectroscopy. This complex was prepared in 87% isolated yield by the addition of potassium cabonate to *trans*-$(PMe_3)_4Ru(Cl)_2$.[21] The carbonate was isolated as a white powder and was identified by ^1H, $^{31}P\{^1H\}$, and $^{13}C\{^1H\}$ NMR, infrared, and mass spectroscopy. An A_2B_2 pattern was observed in the $^{31}P\{^1H\}$ NMR spectrum, with the phosphines located trans to the carbonate ligand resonating downfield from the mutually trans phosphines.

(16) Other examples of C–C cleavage reactions include: (a) Suggs, J. W.; Cox, S. D. *J. Organomet. Chem.* **1981**, *221*, 199. (b) Suggs, J. W.; Jun, C.-H. *J. Am. Chem. Soc.* **1984**, *106*, 3054. (c) Suggs, J. W.; Wovkulich, M. J. *Organometallics* **1985**, *4*, 1101. (d) Suggs, J. W.; Jun, C.-H. *J. Am. Chem. Soc.* **1986**, *108*, 4679. Crabtree, R. H. *Chem. Rev.* **1985**, *85*, 245. (e) Crabtree, R. H.; Dion, R. P.; Gibbone, D. J.; McGrath, D. V.; Holt, E. M. *J. Am. Chem. Soc.* **1986**, *108*, 7222 and references therein. (f) Watson, P. L.; Roe, D. C. *J. Am. Chem. Soc.* **1982**, *104*, 6471. (g) Bunel, E.; Berger, B. J.; Bercaw, J. E. *J. Am. Chem. Soc.* **1988**, *110*, 976.

(17) Hartwig, J. F.; Andersen, R. A.; Bergman, R. G. *J. Am. Chem. Soc.* **1989**, *111*, 2717. (b) Hartwig, J. F.; Bergman, R. G.; Andersen, R. A. *J. Am. Chem. Soc.* **1991**, *113*, 3409.

(18) Statler, J. A.; Wilkinson, G.; Thornton-Pett, M.; Hursthouse, M. B. *J. Chem. Soc., Dalton Trans.* **1984**, 1731.

(19) Mainz, V. V.; Andersen, R. A. *Organometallics* **1984**, *3*, 675.

(20) Hartwig, J. F.; Bergman, R. G.; Andersen, R. A. *J. Organomet. Chem.* **1990**, *394*, 417.

(21) (a) Schmidbaur, H.; Blaschke, G. *Z. Naturforsch., B* **1980**, *356*, 584. (b) Sellmann, D.; Bohlen, E. *Z. Naturforsch. B* **1982**, *37*, 1026.

Scheme IV

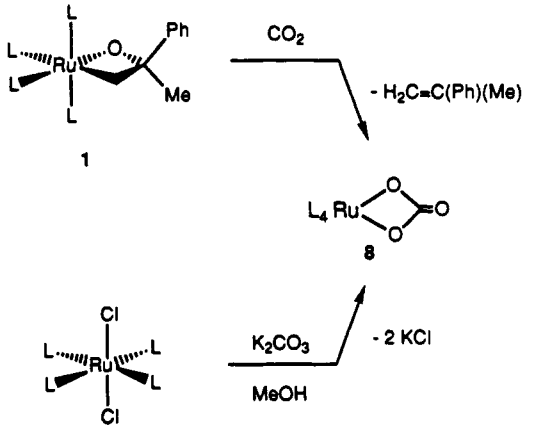

Scheme V

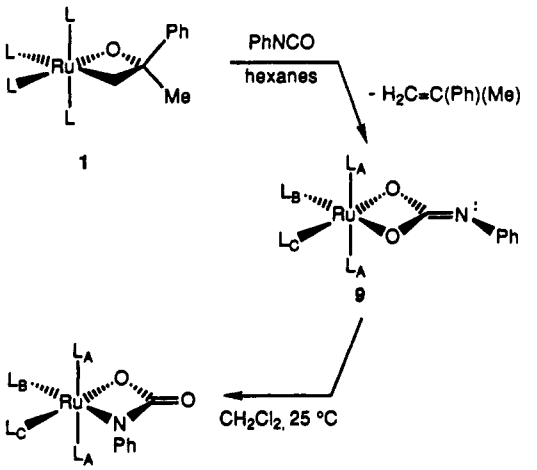

Scheme VI

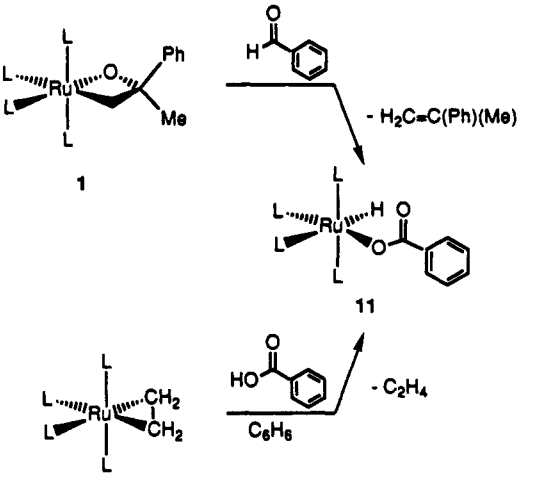

This trend in chemical shift is consistent with that of other $(PMe_3)_4Ru(X)(Y)$ complexes containing ruthenium–heteroatom bonds[14,15,19,20] and reflects the weaker trans influence properties of the carbonate substituent, compared to trimethylphosphine.[22] The carbonate ligand was identified by a singlet resonance at δ 169.2 in the $^{13}C\{^1H\}$ NMR spectrum and by an infrared absorption at 1578 cm^{-1}. A parent peak at m/e = 467 in the FAB mass spectrum was consistent with the assignment of **8** as a monomer.

Reaction of **1** with PhNCO, a compound isoelectronic with CO_2, is shown in Scheme V. Addition of this reagent to **1** led to rapid extrusion of α-methylstyrene and caused precipitation of an initial addition product $(PMe_3)_4Ru(\eta^2\text{-}OC(NPh)O)$ (**9**). This compound was stable in the solid state but rearranged to $(PMe_3)_4Ru(\eta^2\text{-}OC(O)NPh)$ (**10**) in solution. Compound **9** was identified by ^1H, $^{31}P\{^1H\}$, and $^{13}C\{^1H\}$ NMR and infrared spectroscopy of a portion of the crude precipitate, which contained roughly 90% of **9**. The NMR spectra of **9** were temperature dependent. At room temperature an A_2B_2 pattern was observed in the $^{31}P\{^1H\}$ NMR spectrum, requiring rapid inversion at the nitrogen atom. However, at −80 °C this inversion was slow, as indicated by the A_2BC pattern in the $^{31}P\{^1H\}$ NMR spectrum, with similar chemical shifts for P_B and P_C. The methyl groups of the phosphine ligands were not resolved in the ^1H NMR spectrum at this temperature, but they were resolved in the $^{13}C\{^1H\}$ NMR spectrum. The organic substituent was identified by the absorption for the C–N double bond at 1706 cm^{-1} in the infrared spectrum, as well as by the resonance at δ 171.7 in the $^{13}C\{^1H\}$ NMR spectrum.

Attempts to crystallize **9** from either tetrahydrofuran or methylene chloride led to formation of the more stable isomer, $(PMe_3)_4Ru(\eta^2\text{-}OC(O)NPh)$ (**10**). Simply dissolving compound **9** in methylene chloride and warming to 45 °C for 1 h led to clean formation of **10**. This compound was isolated as a yellow/orange powder by diffusion of ether into the methylene chloride solution of **10**, and it was characterized by microanalysis, as well as ^1H, $^{31}P\{^1H\}$, and $^{13}C\{^1H\}$ NMR and infrared spectroscopy. The room temperature $^{31}P\{^1H\}$ NMR spectrum of **10** displayed an A_2BC pattern, with the phosphines located trans to the carboxamide ligand resonating downfield of the mutually trans phosphines. The carboxamide substituent was identified by the carbonyl carbon at δ 167.7 in the $^{13}C\{^1H\}$ NMR spectrum and by the infrared absorption band at 1595 cm^{-1}.

Addition of benzaldehyde to a C_6D_6 solution of **1** followed by heating to 45 °C led to extrusion of α-methylstyrene in 73% yield and provided the hydrido benzoate *cis*-$(PMe_3)_4Ru(H)(OC(O)Ph)$ (**11**) in 53% yield by ^1H NMR spectroscopy (Scheme VI). Compound **11** was prepared independently in 14% isolated yield by the addition of benzoic acid to the ethylene complex $(PMe_3)_4Ru(C_2H_4)$[23] and was characterized by ^1H, $^{31}P\{^1H\}$, and $^{13}C\{^1H\}$ NMR and infrared spectroscopy, as well as by microanalysis. The hydride substituent was identified by the doublet of quartets resonance (one large trans coupling and three indistinguishable cis couplings) at δ −8.21 in the ^1H NMR spectrum and the absorption band at 1826 cm^{-1} in the infrared spectrum. The presence of the benzoate ligand was confirmed by an absorption at 1599 cm^{-1} in the infrared spectrum, a carbonyl resonance in the $^{13}C\{^1H\}$ NMR at δ 172.19, and appropriate resonances for a terminal aryl group in the ^1H and $^{13}C\{^1H\}$ NMR spectrum. An A_2BC pattern in the $^{31}P\{^1H\}$ NMR spectrum established the cis stereochemistry of this complex.

Addition of nonpolarizable unsaturated organic molecules led to no reaction. Addition of *m*-methyl-α-methylstyrene, styrene, isobutylene, dimethylacetylene, or

(22) A trans influence series is given in: Appleton, T. G.; Clark, H. C.; Manzer, L. E. *Coord. Chem. Rev.* **1973**, *10*, 335. Discussion of correlations between trans influence and ^{31}P chemical shifts is found in: (a) Nixon, J. F.; Pidcock, A. *Annu. Rev. NMR Spectrosc.* **1969**, *2*, 345. (b) Verkade, J. M., Quin, L. D., Eds. *Phosphorus-31 NMR Spectroscopy in Stereochemical Analysis*; VCH Publishers: New York, 1987. (c) Meek, D. W.; Mazanec, T. J. *Acc. Chem. Res.* **1981**, *14*, 266.

(23) Wong, W.-K.; Chiu, K. W.; Statler, J. A.; Wilkinson, G.; Motevalli, M.; Hursthouse, M. B. *Polyhedron* **1984**, *3*, 1255.

Scheme VII

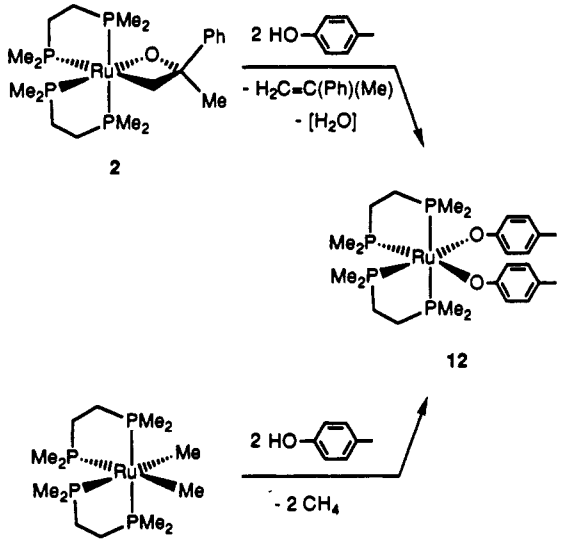

diphenylacetylene to C_6D_6 solutions of **1** led to no change in its room temperature ^1H and $^{31}P\{^1H\}$ NMR spectra. Warming the solutions to 45 °C led to formation of **3** in roughly the same yield as the thermolysis conducted in the absence of the alkene or alkyne.

Reactions of $(DMPE)_2Ru(OC(Me)(Ph)CH_2)$ (2). A comparison of the reactivities of **1** and **2** should provide information on the role of phosphine dissociation in these reactions, since phosphine dissociation in **2** is less facile than in **1**. The most dramatic difference between these two metallacycles was displayed in their thermal chemistry and reactivity toward CO. While **1** forms methane and cyclometalated product **3** at 45 °C, heating C_6D_6 solutions of **2** to 140 °C for 2 days provided ^1H and $^{31}P\{^1H\}$ NMR spectra that were indistinguishable from those of starting material. No formation of methane, α-methylstyrene, or α-methylstyrene oxide was observed. Similarly, metallacycle **2** was stable toward reaction with carbon monoxide. When a solution of **2** was exposed to 2 atm of CO at 85 °C for 24 h, no evidence for ligand substitution or CO insertion was observed by ^1H or $^{31}P\{^1H\}$ NMR spectroscopy.

Addition of 2 equiv of *p*-cresol to crystalline samples of **2** in C_6D_6 at room temperature led to rapid, quantitative formation of α-methylstyrene in addition to the DMPE-substituted bis(cresolate) complex $(DMPE)_2Ru(OC_6H_4\text{-}p\text{-}Me)_2$ (**12**) in 74% yield by ^1H NMR spectroscopy (Scheme VII). Compound **12** was prepared independently in 32% yield by the addition of *p*-cresol to $(DMPE)_2Ru(Me_2)$. Yellow crystals of **12** formed from the reaction mixture, and these were characterized by microanalysis, as well as by ^1H, $^{31}P\{^1H\}$, and $^{13}C\{^1H\}$ NMR and infrared spectroscopy. The cis stereochemistry was indicated by a pair of triplets in the $^{31}P\{^1H\}$ NMR spectrum and by the presence of four methyl groups in the ^1H and $^{13}C\{^1H\}$ NMR spectra. The AA′BB′ pattern in the aryl region of the ^1H NMR spectrum and the presence of two CH and two quaternary resonances in the aryl region of the $^{13}C\{^1H\}$ NMR spectrum demonstrated the η^1-binding mode of the cresolate substituents. Because the preparation of starting dimethyl compound **12** was reported in 1963 without the aid of NMR spectroscopy,[25] its ^1H, $^{31}P\{^1H\}$, and $^{13}C\{^1H\}$ NMR spectroscopic data are included in Tables VIII–X.

The reaction of metallacycle **2** with carbon dioxide in C_6D_6 at room temperature led to extrusion of α-methylstyrene (96%) and precipitation of the DMPE-substituted ruthenium carbonate $(DMPE)_2Ru(CO_3)$ (**13**) (Scheme VIII). The carbonate complex was dissolved by adding

Scheme VIII

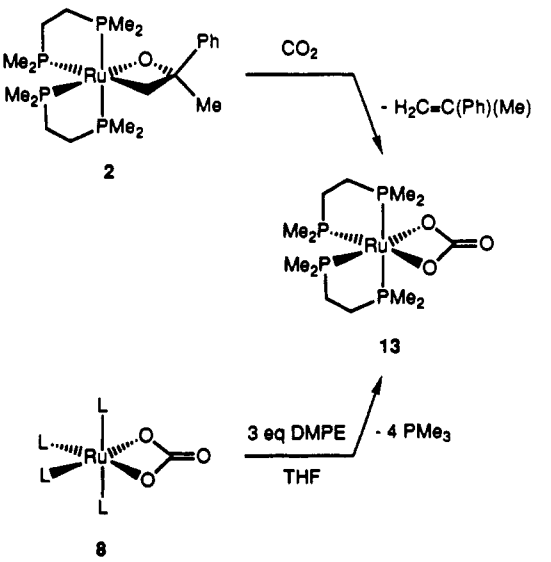

Scheme IX

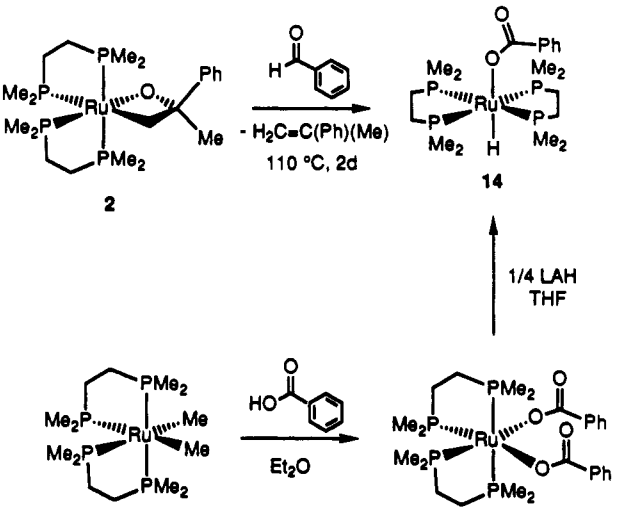

CD_2Cl_2 to the reaction solution containing an internal standard, and ^1H NMR spectroscopy of the homogeneous solution showed that **13** was formed in quantitative yield. This compound was prepared independently in 34% yield and spectroscopically characterized by adding an excess of DMPE to a methanol solution of the PMe_3-substituted carbonate **8**. Compound **13** was isolated as a white powder; its most revealing spectroscopic features were an IR absorption band at 1566 cm^{-1} and a $^{13}C\{^1H\}$ NMR resonance at δ 167.5, corresponding to the carbonate substituent. The two DMPE ligands were identified by two triplet resonances in the $^{31}P\{^1H\}$ NMR spectrum in the same chemical shift region as the other DMPM complexes prepared in this study and by the four methyl resonances observed in the ^1H and $^{13}C\{^1H\}$ NMR spectra.

Reaction of **2** with 1 equiv of benzaldehyde, followed by heating to 110 °C for 2 days, led to formation of α-methylstyrene in quantitative yield and hydrido benzoate *trans*-$(DMPE)_2Ru(H)(OC(O)Ph)$ (**14**) in 57% yield (Scheme IX), a transformation analogous to that observed upon addition of benzaldehyde to the PMe_3-substituted metallacycle **1**. However, the reaction with compound **2** required prolonged heating at elevated temperatures. Again the product was prepared independently, this time in 53% isolated yield by addition of 0.25 equiv of lithium aluminum hydride to the bis(benzoate) complex **15**. White, crystalline samples of compound **14** were obtained by

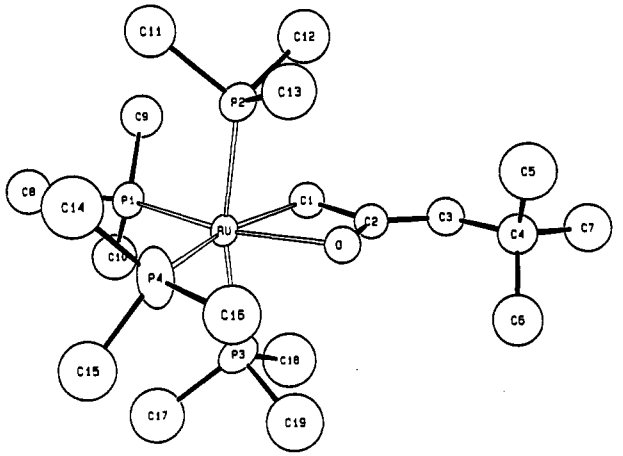

Figure 1. ORTEP drawing of 15.

crystallization from ether and were characterized by microanalysis, as well as ^1H, $^{31}P\{^1H\}$, and $^{13}C\{^1H\}$ NMR and infrared spectroscopy. The hydride substituent was identified by the quintet ^1H NMR resonance at δ −22.47 and by the absorption at 1907 cm^{-1} in the infrared spectrum. The presence of the benzoate ligand was confirmed by the infrared absorption at 1601 cm^{-1}, by the $^{13}C\{^1H\}$ NMR resonance at δ 170.42, and by the presence of the appropriate resonances for a terminal phenyl group in the ^1H and $^{13}C\{^1H\}$ NMR spectra. The trans stereochemistry was indicated by the singlet resonance in the $^{31}P\{^1H\}$ NMR spectrum, the presence of two methyl groups in the ^1H and $^{13}C\{^1H\}$ NMR spectra, and the quintet hydride resonance. The starting bis(benzoate) complex was prepared in 60–70% isolated yield upon addition of 2 equiv of benzoic acid to either the naphthyl hydride complex *cis*-$(DMPE)_2Ru(C_{10}H_7)(H)$[24] or the dimethyl complex *cis*-$(DMPE)Ru(Me)_2$[25] and was spectroscopically characterized. Data for this complex are included in Tables VIII–X.

Because C_6D_6 solutions of metallacycle **2** were unchanged upon heating to temperatures below 140 °C, compound **2** could be treated with alkenes and alkynes at higher temperatures than those employed with the PMe_3 metallacycle **1**. However, even heating samples of **2** to 135 °C for 24 h in the presence of *m*-methyl-α-methylstyrene, styrene, dimethylacetylene, or diphenyl acetylene did not lead to incorporation of these substrates into the metallacycle portion of the molecule. No change in the ^1H and $^{31}P\{^1H\}$ NMR spectra of these reaction mixtures was observed under these conditions.

Structure and Reactions of $(PMe_3)_4Ru(\eta^2\text{-}OC(CHCMe_3)CH_2)$ (15). We have not been able to crystallographically characterize a ruthenium oxametallacyclobutane containing two sp^3 hybridized carbons in the ring. However, we were able to structurally characterize the related sp^2 carbon-containing system $(PMe_3)_4Ru(OC(CHCMe_3)CH_2)$ (**15**). This oxametallacyclobutane complex, which has a *tert*-butylmethylene substituent in the β-position, was prepared by the addition of 2 equiv of the potassium enolate of 4,4-dimethyl-2-pentanone to the acetate chloride complex $(PMe_3)_4Ru(OAc)(Cl)$, as described in the previous paper.[14c] Single crystals suitable for an X-ray diffraction study were obtained by cooling a pentane solution of **15** to −40 °C. The structure was solved by Patterson methods and refined by standard least squares and Fourier techniques. An ORTEP drawing of the molecule is shown in Figure 1. Crystal and data collection parameters are provided in Table I; intramolecular distances and angles are provided in Tables II and III. The compound crystallized in space group $P2_1/n$, with no unusually short intermolecular distances. The molecule possesses a pseudooctahedral geometry, with the metallacycle occupying two cis sites. The metallacyle portion is flat; the dihedral angle in the ring is 1.9°. The *tert*-butyl group lies far from the phosphine ligands. All nonbonding distances between the phosphine methyl groups and the *tert*-butyl methyl groups are significantly longer than 4 Å. The C(2)–O bond length is 1.347 (7) Å, similar to the C–O bond length in enols, and the C2–C3 distance is 1.364 (9) Å, also similar to the C=C distances in enol tautomers and slightly longer than isolated C=C bonds.[26] The C(1)–C(2) distance is 1.547 (9) Å, consistent with a localized carbon–carbon single bond.[26] The phosphine ligands oc-

Table I. Crystal and Data Collection Parameters[a]

	15	17	18
temp, °C	−85	−90	−90
empirical formula	$RuP_4OC_{19}H_{48}$	$RuP_4OC_{15}H_{42}$	$RuP_3OC_{12}H_{31}$
fw	517.6	463.5	385.4
cryst size, mm	0.15 × 0.13 × 0.55	0.20 × 0.30 × 0.60	0.12 × 0.26 × 0.27
space group	$P2_1/n$	$P2_1/n$	$Pnma$
a, Å	9.785 (3)	9.337 (2)	14.027 (2)
b, Å	19.306 (6)	15.615 (3)	15.175 (3)
c, Å	14.715 (6)	15.536 (1)	8.792 (1)
α, deg	90.0	90.0	90.0
β, deg	102.73 (2)	102.025 (15)	90.0
γ, deg	90.0	90.0	90.0
V, Å^3	2711.4 (24)	2215.6 (13)	1871.4 (8)
Z	4	4	4
d_{calc}, g cm^{-3}	1.27	1.43	1.88
μ_{calc}, cm^{-1}	8.1	9.8	14.6
rflns measd	$+h, +k, \pm l$	$+h, k, \pm l$	$+h, +k, +l$
scan width	$\Delta\theta$ = 0.75 + 0.35 tan θ	$\Delta\theta$ = 0.85 + 0.35 tan θ	$\Delta\theta$ = 1.20 + 0.35 tan θ
scan speed (θ, deg/min)	6.70	6.70	6.70
setting angles (2θ, deg)[b]	24–28	24–28	22–26

[a] Parameters common to all structures: radiation, Mo Kα; monochromator, highly oriented graphite (2θ = 12.2°); detector, crystal scintillation counter, with PHA; scan type, θ–2θ; background, measured over 0.25($\Delta\theta$) added to each end of the scan; vertical aperture = 3.0 mm; horizontal aperture = 2.0 + 1.0 tan θ mm; intensity standards, measured every hour of X-ray exposure time; orientation, three reflections were checked after every 200 measurements; crystal orientation was redetermined if any of the reflections were offset from their predicted positions by more than 0.1°. [b] Unit cell parameters and their esd's were derived by a least-squares fit to the setting angles of the unresolved Mo Kα components of 24 reflections with the given 2θ range. In this and all subsequent tables the esd's of all parameters are given in parentheses, right justified to the least significant digit(s) of the reported value.

Table II. Intramolecular Distances for 15

atom 1	atom 2	dist, Å	atom 1	atom 2	dist, Å
Ru	P1	2.250 (2)	P1	C8	1.849 (8)
Ru	P2	2.345 (2)	P1	C9	1.854 (8)
Ru	P3	2.341 (2)	P1	C10	1.839 (9)
Ru	P4	2.335 (2)	P2	C11	1.859 (9)
Ru	O	2.146 (4)	P2	C12	1.838 (10)
Ru	C1	2.158 (7)	P2	C13	1.854 (9)
C2	O	1.347 (7)	P3	C17	1.891 (11)
C2	C1	1.547 (9)	P3	C18	1.861 (11)
C2	C3	1.364 (9)	P3	C19	1.860 (11)
C3	C4	1.526 (9)	P4	C14	1.924 (11)
C4	C5	1.523 (12)	P4	C15	1.834 (10)
C4	C6	1.524 (11)	P4	C16	1.864 (10)
C4	C7	1.561 (10)			

(24) Chatt, J.; Davidson, J. M. *J. Chem. Soc.* **1965**, 843.
(25) Chatt, J.; Hayter, R. G. *J. Chem. Soc.* **1963**, 6017.
(26) Allen, F. H.; Kennard, O.; Watson, D. G.; Brammer, L.; Orpen, D. G.; Taylor, R. *J. Chem. Soc., Perkin Trans. 2* **1987**, S1.

Table III. Intramolecular Angles for 15

atom 1	atom 2	atom 3	angle, deg
P1	Ru	P2	94.59 (7)
P1	Ru	P3	96.14 (8)
P1	Ru	P4	101.79 (7)
P1	Ru	O	161.74 (12)
P1	Ru	C1	94.96 (19)
P2	Ru	P3	167.78 (7)
P2	Ru	P4	91.55 (9)
P2	Ru	O	82.71 (13)
P2	Ru	C1	87.08 (19)
P3	Ru	P4	91.98 (10)
P3	Ru	O	85.27 (13)
P3	Ru	C1	86.17 (20)
P4	Ru	O	96.34 (13)
P4	Ru	C1	163.25 (18)
O	Ru	C1	66.92 (21)
Ru	O	C2	94.6 (4)
Ru	C1	C2	88.5 (4)
O	C2	C1	110.0 (5)
O	C2	C3	125.5 (6)
C1	C2	C3	124.5 (6)
C2	C3	C4	125.5 (6)
C3	C4	C5	110.7 (7)
C3	C4	C6	112.5 (6)
C3	C4	C7	107.0 (6)
C5	C4	C6	110.5 (7)
C5	C4	C7	108.9 (7)
C6	C4	C7	107.1 (6)
Ru	P1	C8	121.9 (3)
Ru	P1	C9	114.9 (3)
Ru	P1	C10	118.7 (3)
C8	P1	C9	101.9 (4)
C8	P1	C10	97.9 (4)
C9	P1	C10	97.3 (4)
Ru	P2	C11	122.6 (3)
Ru	P2	C12	118.8 (3)
Ru	P2	C13	113.4 (3)
C11	P2	C12	99.8 (4)
C11	P2	C13	99.8 (4)
C12	P2	C13	98.3 (4)
Ru	P3	C17	123.5 (3)
Ru	P3	C18	117.8 (4)
Ru	P3	C19	111.8 (3)
C17	P3	C18	99.0 (5)
C17	P3	C19	100.3 (5)
C18	P3	C19	101.0 (5)
Ru	P4	C14	122.6 (3)
Ru	P4	C15	122.1 (3)
Ru	P4	C16	111.4 (3)
C14	P4	C15	95.4 (5)
C14	P4	C16	101.7 (4)
C15	P4	C16	99.7 (4)

cupy the remaining four sites of the octahedron, and the bond lengths are in the range found in ruthenium compounds of similar structure.[17b,27] The Ru–P(1) distance trans to the oxygen is significantly shorter (2.250 (2) Å) than the Ru–P(2) distance trans to the methylene (2.345 (2) Å) or the Ru–P(3,4) distance of the mutually trans phosphines (2.341 (2) and 2.335 (2) Å).

Extrusion of *tert*-butylallene from **15** upon addition of protic reagents would be analogous to the reactivities of metallacycles **1** and **2**. However, addition of 2 equivalents of *p*-cresol to a C_6D_6 solution of **15** led to formation of both the free ketone 4,4-dimethyl-2-pentanone and the bis(cresolate) complex **7** in quantitative yield (Scheme X). ^{1}H NMR spectroscopic identification of the organic product was confirmed by comparing the GC retention time with that of an authentic sample.

Although **15** does not extrude alkene by a C–O bond cleavage process analogous to that observed with **1** and **2**, it does undergo a different type of ketone carbon–carbon

(27) Hartwig, J. F.; Andersen, R. A.; Bergman, R. G. *Organometallics* **1991**, *10*, 1875.

Scheme X

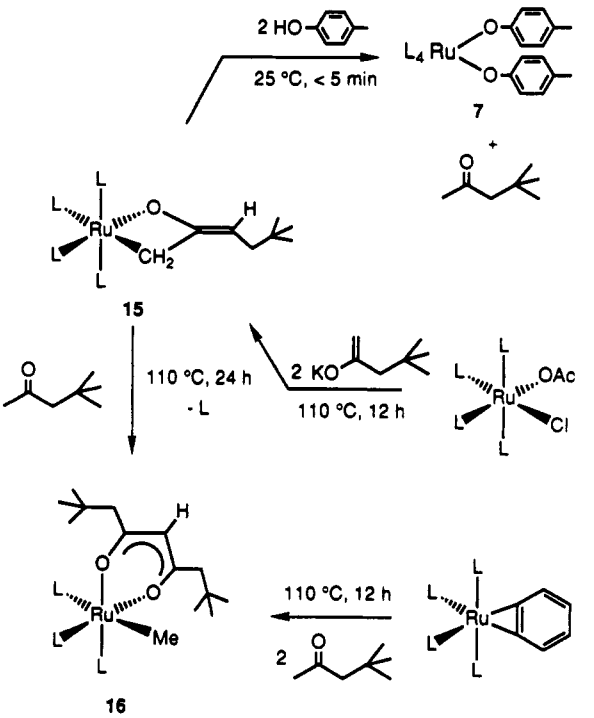

Table IV. Intramolecular Distances for 17

atom 1	atom 2	dist, Å	atom 1	atom 2	dist, Å
Ru	P1	2.308 (1)	P1	C6	1.827 (5)
Ru	P2	2.324 (1)	P2	C7	1.835 (5)
Ru	P3	2.358 (1)	P2	C8	1.836 (5)
Ru	P4	2.352 (1)	P2	C9	1.837 (5)
Ru	C1	2.217 (4)	P3	C10	1.850 (5)
Ru	C2	2.222 (5)	P3	C11	1.814 (5)
C1	C3	1.468 (7)	P3	C12	1.814 (6)
C2	C3	1.459 (7)	P4	C13	1.838 (5)
C3	O1	1.261 (6)	P4	C14	1.839 (5)
P1	C4	1.838 (5)	P4	C15	1.836 (5)
P1	C5	1.842 (5)			

bond cleavage. Addition of 4,4-dimethyl-2-pentanone followed by heating to 110 °C for 12 h led to formation of the di-*tert*-butyl-substituted acetylacetonate complex **16** in 77% yield by ^{1}H NMR spectroscopy. This product is again the result of a carbon–carbon bond formation and a subsequent carbon–carbon bond cleavage process. Compound **16** was more conveniently obtained by the addition of 2 equiv of the potassium enolate of 4,4-dimethyl-2-pentanone to the acetate chloride complex $(PMe_3)_4Ru(OAc)(Cl)$,[19] which generated reactants **15** and free ketone in situ. Alternatively, compound **16** was synthesized on a preparative scale by the addition of 2 equiv of 4,4-dimethyl-2-pentanone to $(PMe_3)_4Ru(\eta^2\text{-}C_6H_4)$,[15] followed by heating to 110 °C for 24 h. Yellow crystals of **16** were isolated from this reaction in 35% yield, and these were characterized by microanalysis as well as by ^{1}H, ^{31}P{^{1}H}, and ^{13}C{^{1}H} NMR and infrared spectroscopy. In addition, the organic ligand was identified by treating a solution of **16** with a slight excess of concentrated HCl to form free *tert*-butylacetylacetone in quantitative yield by ^{1}H NMR spectroscopy. The free ketone was characterized by comparing its GC retention time and ^{1}H NMR spectrum with those of an authentic sample. The bound organic ligand was identified by the presence of two infrared bands at 1576 and 1561 cm^{-1}, a methine ^{1}H NMR resonance at δ 5.15, and two chemically equivalent neopentyl groups, each exhibiting an AB methylene pattern in the ^{1}H NMR spectrum. An A_2B pattern in the ^{31}P{^{1}H} NMR

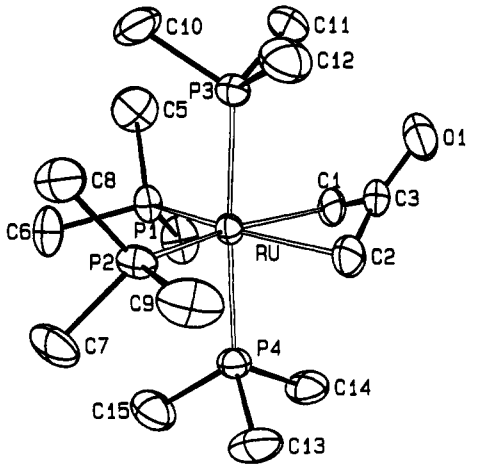

Figure 2. ORTEP drawing of 17.

Table V. Intramolecular Angles for 17

atom 1	atom 2	atom 3	angle, deg
P1	Ru	P2	103.23 (4)
P1	Ru	P3	92.50 (4)
P1	Ru	P4	91.72 (4)
P1	Ru	C1	92.98 (13)
P1	Ru	C2	158.11 (14)
P2	Ru	P3	90.78 (4)
P2	Ru	P4	89.77 (4)
P2	Ru	C1	163.79 (13)
P2	Ru	C2	98.15 (14)
P3	Ru	P4	175.50 (5)
P3	Ru	C1	88.23 (13)
P3	Ru	C2	91.86 (13)
P4	Ru	C1	90.00 (13)
P4	Ru	C2	83.65 (13)
C1	Ru	C2	65.72 (18)
Ru	C1	C3	83.5 (3)
Ru	C2	C3	83.5 (3)
O1	C3	C1	124.1 (5)
O1	C3	C2	123.0 (5)
C1	C3	C2	110.8 (4)
Ru	P1	C4	115.36 (18)
Ru	P1	C5	120.59 (19)
Ru	P1	C6	121.36 (17)
C4	P1	C5	95.6 (3)
C4	P1	C6	101.74 (24)
C5	P1	C6	97.5 (3)
Ru	P2	C7	121.99 (17)
Ru	P2	C8	122.41 (16)
Ru	P2	C9	113.67 (20)
C7	P2	C8	95.93 (25)
C7	P2	C9	100.1 (3)
C8	P2	C9	98.0 (3)
Ru	P3	C10	121.42 (18)
Ru	P3	C11	118.50 (18)
Ru	P3	C12	115.16 (19)
C10	P3	C11	97.82 (24)
C10	P3	C12	100.6 (3)
C11	P3	C12	99.4 (3)
Ru	P4	C13	117.94 (18)
Ru	P4	C14	117.66 (17)
Ru	P4	C15	122.70 (19)
C13	P4	C14	98.26 (24)
C13	P4	C15	97.4 (3)
C14	P4	C15	98.08 (25)

spectrum was consistent with the presence of equivalent neopentyl groups. The metal-bound methyl group was identified by a doublet of triplets resonance at δ 0.34 in the ^{1}H NMR spectrum, integrating to three protons, and a CH_3 resonance (confirmed by a DEPT pulse sequence) with a similar splitting pattern in the $^{13}C\{^1H\}$ NMR spectrum at δ 4.83.

Structure and Reactions of $(PMe_3)_4Ru((CH_2)_2CO)$ (17). The compound $(PMe_3)_4Ru[(CH_2)_2CO]$ (17), a second metallacycle formed by metalation of a ruthenium enolate, has been prepared as described in the previous paper.[14c] Unlike its analogue, compound **15**, the acetone dianion complex **17** does not contain a ruthenium–oxygen bond; rather, the complex is bound through the two CH_2 groups. A single crystal suitable for an X-ray diffraction study was obtained by cooling a pentane solution to −40 °C. The structure was solved by Patterson methods and refined by standard least-squares and Fourier techniques. An ORTEP drawing of the molecule is shown in Figure 2. Crystal and data collection parameters are provided in Table I; intramolecular distances and angles are provided in Tables IV and V. The compound crystallized in space group $P2_1/n$, with no unusually short intermolecular distances.

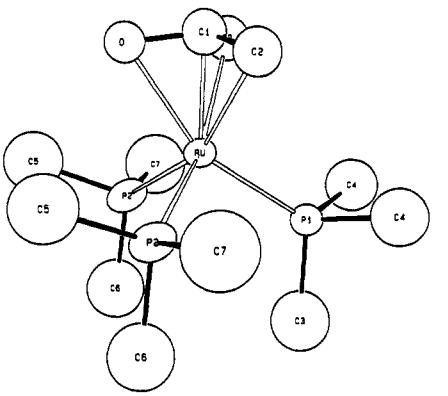

Figure 3. ORTEP drawing of 18.

Scheme XI

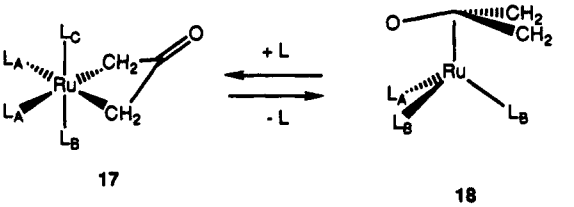

17 18

Table VI. Intramolecular Distances for 18

atom 1	atom 2	dist, Å	atom 1	atom 2	dist, Å
Ru	P1	2.237 (4)	C1	C2	1.388 (13)
Ru	P2	2.286 (3)	P1	C3	1.790 (24)
Ru	O	2.224 (10)	P1	C4	1.820 (15)
Ru	C1	1.985 (19)	P2	C5	1.795 (17)
Ru	C2	2.265 (12)	P2	C6	1.790 (17)
C1	O	1.325 (17)	P2	C7	1.828 (20)

Table VII. Intramolecular Angles for 18

atom 1	atom 2	atom 3	angle, deg
P1	Ru	P2	96.90 (11)
P1	Ru	O	157.6 (3)
P1	Ru	C1	121.4 (5)
P1	Ru	C2	100.1 (3)
P2	Ru	P2	98.62 (16)
P2	Ru	O	97.68 (19)
P2	Ru	C1	119.0 (3)
P2	Ru	C2	156.3 (3)
O	C1	C2	115.6 (9)
C2	C1	C2	123.2 (16)
Ru	P1	C3	120.8 (8)
Ru	P1	C4	117.3 (5)
C3	P1	C4	101.6 (7)
C4	P1	C4	93.6 (10)
Ru	P2	C5	111.1 (6)
Ru	P2	C6	124.9 (6)
Ru	P2	C7	115.8 (6)
C5	P2	C6	103.7 (7)
C5	P2	C7	101.0 (8)
C6	P2	C7	97.1 (8)

Table VIII. ^{1}H NMR Spectroscopic Data

compound	δ, ppm	mult[a]	J, Hz	int	assignment[b]
$(PMe_3)_4Ru(OC(CH_2)C_6H_4)$ (3)[d]	1.02	t	3.0	18	*trans*-PMe_3
	1.42	d	6.9	9	*cis*-PMe_3
	1.45	d	6.0	9	*cis*-PMe_3
	3.39	d	1.2	1	$(OC(CH_aH_b)C_6H_4)$
	3.95	br s		1	$(OC(CH_aH_b)C_6H_4)$
	6.61	tq	7.3, 1.0	1	$(OC(CH_2)C_6H_4)$
	6.63	t	7.7	1	
	7.11	dt	7.6, 1.6	1	
	7.46	m		1	
$(CO)(PMe_3)_3Ru(OC(Me)(Ph)CH_2C(O))$ (6)[e]	0.87	d	7.3	9	PMe_3
	1.02	d	6.1	9	
	1.25	d	7.2	9	
	1.47	s		3	$(OC(Me)(Ph)CH_2C(O))$
	2.98	d	15.5	1	$(OC(Me)(Ph)CH_aH_bC(O))$
	3.09	dd	15.5, 4.0	1	$(OC(Me)(Ph)CH_aH_bC(O))$
	7.12	t	7.2	1	$(OC(Me)(Ph)CH_2C(O))$
	7.29	t	7.6	2	
	8.82	d	7.8	2	
cis-$(PMe_3)_4Ru(OC_6H_4$-*p*-$Me)_2$ (7)[e]	0.96	d	7.7	18	*cis*-PMe_3
	1.14	t	3.1	18	*trans*-PMe_3
	2.40	s		6	$(OC_6H_4$-*p*-$Me)_2$
	7.04	d	8.4	4	$(OC_{6H4}$-*p*-$Me)_2$
	7.22	d	8.3	4	
$(PMe_3)_4Ru(CO_3)$ (8)[f]	1.40	t	3.3	18	*trans*-PMe_3
	1.40	m		18	*cis*-PMe_3
$(PMe_3)_4Ru(OC(NPh)O)$ (9)[g]	1.37	m		36	*cis*- and *trans*-PMe_3
	6.55	t	7.7	1	(OC(N*Ph*)O)
	6.96	t	7.3	2	
	7.22	d	7.5	2	
$(PMe_3)_4Ru(OC(O)NPh)$ (10)[h]	1.28	t	2.8	18	*trans*-PMe_3
	1.44	d	7.9	9	*cis*-PMe_3
	1.47	d	7.4	9	*cis*-PMe_3
	6.53	t	7.1	1	(OC(O)N*Ph*)
	7.03	t	7.7	2	
	7.27	d	7.9	2	
cis-$(PMe_3)_4Ru(H)(OC(O)Ph)$ (11)[e]	−8.21	dq	101, 25.7	1	RuH
	1.00	d	7.4	9	*cis*-PMe_3
	1.28	d	5.4	9	*cis*-PMe_3
	1.32	br s		18	*trans*-PMe_3
	7.21	t	6.8	1	(OC(O)*Ph*)
	7.30	t	7.5	2	
	8.48	d	7.7	2	
cis-$(DMPE)_2Ru(Me)_2$[e]	−0.36	m		6	RuMe
	0.95	d	4.6	6	$Me_2PCH_2CH_2PMe_2$
	1.02	d	5.9	6	
	1.04	s		6	
	1.18	t	2.9	6	
	0.87	m		2	$Me_2PCH_2CH_2PMe_2$
	1.23	m		2	
	1.38	m		4	
cis-$(DMPE)_2Ru(OC_6H_4$-*p*-$Me)_2$ (12)[d]	1.24	s		6	$Me_2PCH_2CH_2PMe_2$
	1.24	t	3.7	6	
	1.37	t	3.5	6	
	1.44	d	9.3	6	
	1.68	m		8	$Me_2PCH_2CH_2PMe_2$
	2.06	s		6	$(OC_6H_4$-*p*-*Me*)
	6.50	d	8.5	4	$(OC_6H_4$-*p*-Me)
	6.55	d	8.5	4	
$(DMPE)_2Ru(CO_3)$ (13)[h]	1.26	d	7.0	6	$Me_2PCH_2CH_2PMe_2$
	1.28	d	4.1	6	
	1.32	t	3.6	6	
	1.44	t	2.3	6	
	1.7–1.9	m		4	$Me_2PCH_2CH_2PMe_2$
	1.9–2.05	m		4	
cis-$(DMPE)_2Ru(OC(O)Ph)_2$[h]	1.16	d	8.4	6	$Me_2PCH_2CH_2PMe_2$
	1.35	d	6.8	6	
	1.76	s		6	
	1.84	s		6	
	1.3–1.5	m		8	$Me_2PCH_2CH_2PMe_2$
	7.22	m		3	(OC(O)*Ph*)
	7.83	d	7.4	2	
trans-$(DMPE)_2Ru(H)(OC(O)Ph)$ (14)[e]	−22.47	quin	21.5	1	RuH
	1.14	s		12	$Me_2PCH_2CH_2PMe_2$
	1.36	s		12	
	1.34	m		4	$Me_2PCH_2CH_2PMe_2$
	1.97	m		4	
	7.19	t	7.2	1	(OC(O)*Ph*)

Table VIII (Continued)

compound	δ, ppm	mult[a]	*J*, Hz	int	assignment[b]
trans-$(DMPE)_2Ru(H)(OC(O)Ph)$ (14)[e]	7.29	t	7.3	2	
	8.41	d	7.2	2	
$(PMe_3)_3Ru(CH(C(O)CH_2CMe_3)_2)(Me)$ (16)[e]	0.34	dt	5.1, 3.4	3	RuMe
	1.06	d	5.6	9	PMe_3
	1.16	d	6.9	18	PMe_3
	1.17	s		18	$(CH(C(O)CH_2CMe_3)_2)$
	1.97	d	11.4	2	$(CH(C(O)CH_2CMe_3)_2)$
	2.10	d	11.4	2	$(CH(C(O)CH_2CMe_3)_2)$
	5.15	s		1	$(CH(C(O)CH_2CMe_3)_2)$
$(PMe_3)_4Ru(OC(Me)CHC(Me)CH$ (19)[e]	0.98	d	7.0	9	*cis*-PMe_3
	1.16	d	5.7	9	*cis*-PMe_3
	1.18	t	2.9	18	*trans*-PMe_3
	2.03	s		3	$(OC(Me)CHC(Me)CH)$
	2.34	s		3	$(OC(Me)CHC(Me)CH)$
	4.88	d	1.9	1	$(OC(Me)CHC(Me)CH)$
	6.22	dm	11.1	1	$(OC(Me)CHC(Me)CH)$
$(PMe_3)_4Ru(OC(O)OC(CMe_3)CH)$ (21)[d]	0.79	d	7.5	9	*cis*-PMe_3
	1.04	d	5.8	9	*cis*-PMe_3
	1.06	t	1.9	18	*trans*-PMe_3
	1.44	s		9	$(OC(O)OC(CMe_3)CH)$
	5.34	dt	7.1, 2.6	1	$(OC(O)OC(CMe_3)CH)$

[a] The multiplicities triplet and doublet, when applied to the PMe_3 and DMPE resonances, are apparent splitting patterns. Accordingly, the values reported for *J* do not necessarily reflect true coupling constants; for example, the tabulated coupling constant in a triplet is the separation between the central line and the outer lines. [b] The assignment *trans*-PMe_3 refers to the mutually trans phosphine ligands; the other two phophines are assigned as *cis*-PMe_3. [c] THF-d_8, −40 °C. [d] THF-d_8, 20°C. [e] C_6D_6, 20 °C. [f] Methanol-d_4, 20 °C. [g] CD_2Cl_2, −62 °C. [h] CD_2Cl_2, 20 °C.

Although both complexes contain an sp^2-hybridized carbon at the β-position of the ring, the solid-state structure of **17** is markedly different from that of the planar *tert*-butyl-substituted analogue **15**. Compound **17** contains two ruthenium–carbon linkages and a large dihedral angle of 45.6 (5)° for the metallacycle, although the Ru–O distance remains long. The C(3)–O distance is 1.261 (3) Å, significantly longer than the average C=O bond length in cyclobutanones, while the C(1)–C(3) and C(2)–C(3) distances are 1.468 (7) and 1.459 (7) Å. These values are significantly shorter than typical carbon–carbon C(O)–C distances in ketones, including the average of those in cyclobutanones, 1.529 Å.[26] The distances between the carbonyl oxygen atom of the organic substituent and the two nearest phosphine methyl groups are 2.977 (6) and 3.133 (7) Å, much shorter than the closest interactions of the organic substituent of **15** with the trimethylphosphine ligands.

Compound **17** underwent facile phosphine ligand dissociation to form the oxatrimethylenemethane complex **18**, as shown in Scheme XI. Tris(phosphine) compound **18** was isolated by removing solvent and excess PMe_3 at 25 °C under reduced pressure, followed by sublimation. The ^1H NMR spectrum displayed two methylene resonances but the $^{13}C\{^1H\}$ NMR spectrum exhibited only one CH_2 resonance, indicating that the two protons on each carbon are inequivalent. The $^{31}P\{^1H\}$ NMR spectrum displayed an A_2B pattern, consistent with loss of one PMe_3 ligand from **17**.

An X-ray diffraction study was conducted on a single crystal of **18**, obtained by sublimation in a sealed tube over a period of 2 weeks at 55 °C. The structure was solved by Patterson methods and refined by standard least-squares and Fourier techniques. An ORTEP drawing of the molecule is shown in Figure 3. Crystal and data collection parameters are provided in Table I; intramolecular distances and angles are provided in Tables VI and VII. The compound crystallized in space group $P2_1/n$, with no unusually short intermolecular distances. The study was hampered by a poor data set, due to poor crystal quality and disorder between the methylene and oxygen positions in the organic ligand. As a result, the data were used principally to confirm the connectivity of **18**, rather than to provide detailed information concerning the bonding mode. Nevertheless, certain overall features of the molecule remained unambiguous. The organic substituent and the three phosphine ligands adopt a staggered conformation, making the overall geometry pseudooctahedral. In addition, the oxatrimethylenemethane substituent is bound in an η^4-fashion. The central carbon is located above the plane of the other three atoms, although the Ru–C(1) distance (1.99 (2) Å) remains significantly shorter than the two Ru–C(2) (2.27 (1) Å) distances and the Ru–O distances (2.22 (1) Å).

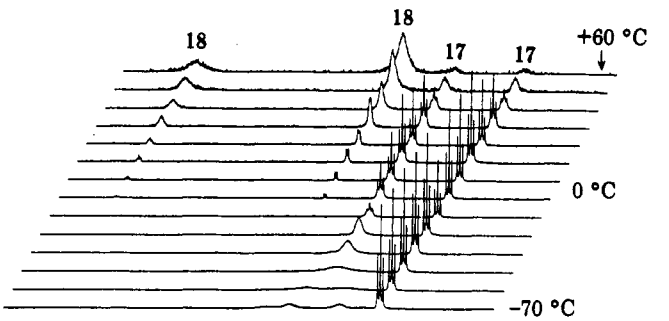

Figure 4. Variable-temperature $^{31}P\{^1H\}$ NMR spectra of **17** ⇌ **18** + PMe_3.

$^{31}P\{^1H\}$ NMR spectroscopy of a toluene-d_8 solution prepared from a crystalline sample of compound **17** and 1 equiv of phosphine demonstrated that compounds **17** and **18** exist in equilibrium under these conditions. Figure 4 displays a stacked plot of the $^{31}P\{^1H\}$ NMR spectra of such a solution between the temperatures −70 and 60 °C. At temperatures below −20 °C, only the complex containing four phosphines (**17**) was observed; while at 60 °C, **18** was the predominant species. Although interconversion of **17** and **18** did not occur rapidly enough to average their distinctive $^{31}P\{^1H\}$ NMR signals, equilibration of the two compounds was complete after less than 5 min even at −20 °C.

Because of the instability of compound **17**, only a few reactivity studies with this complex were attempted. For example, a solution of **17** and free acetone, generated in situ by addition of 2 equiv of the potassium enolate of

Table IX. $^{13}C\{^1H\}$ NMR Spectroscopic Data

compound	δ, ppm	mult[a]	J, Hz	assignment[b]
$(PMe_3)_4Ru(OC(CH_2)C_6H_4)$ (3)[d]	19.40	td	12.6, 2.6	*trans*-PMe_3
	22.28	dt	17.0, 1.7	*cis*-PMe_3
	25.23	dm	23.6	*cis*-PMe_3
	72.90	s		$(OC(CH_2)C_6H_4)$
	120.68	d	1.3	$(OC(CH_2)C_6H_4)$
	122.61	d	1.4	
	125.23	m		
	141.27	m		
	152.86	d	3.1	
	176.60	dm	7.7	$(OC(CH_2)C_6H_4)$
	177.71	dq	65.0, 8.2	$(OC(CH_2)C_6H_4)$
$(CO)(PMe_3)_3Ru_3(OC(Me)(Ph)CH_2C(O))$ (6)[e]	17.76	dt	23, 4	PMe_3
	18.14	dt	15, 3	
	18.20	dt	4, 4	
	38.08	s		$(OC(Me)(Ph)CH_2C(O))$
	74.65	d	20.0	$(OC(Me)(Ph)CH_2C(O))$
	76.82	d	5.8	$(OC(Me)(Ph)CH_2C(O))$
	124.24	s		$(OC(Me)(Ph)CH_2C(O))$
	126.62	s		
	127.52	s		
	157.65	s		
	201.36	m		RuCO
	268.31	dm	100.1	$(OC(Me)(Ph)CH_2C(O))$
cis-$(PMe_3)_4Ru(OC_6H_4$-*p*-$Me)_2$ (7)[d]	18.56	t	12.6	*trans*-PMe_3
	22.57	m		*cis*-PMe_3
	20.75	s		$(OC_6H_4$-*p*-$Me)_2$
	118.36	s		$(OC_6H_4$-*p*-$Me)_2$
	120.66	s		
	129.68	s		
	169.41	s		
$(PMe_3)_4Ru(CO_3)$ (8)[f]	16.98	t	13	*trans*-PMe_3
	22.48	m		*cis*-PMe_3
	169.22	s		$RuCO_3$
$(PMe_3)_4Ru(OC(NPh)O)$ (9)[g]	15.88	t	13.1	*trans*-PMe_3
	21.18	d	23.3	*cis*-PMe_3
	21.43	d	26.2	*cis*-PMe_3
	116.34	s		$(OC(NPh)O)$
	122.55	s		
	127.66	s		
	152.69	s		
	171.66	s		$(OC(NPh)O)$
$(PMe_3)_4Ru(OC(O)NPh)$ (10)[h]	18.31	t	13.1	*trans*-PMe_3
	22.21	dt	26.1, 2.0	*cis*-PMe_3
	25.57	dq	26.4, 2.1	*cis*-PMe_3
	116.26	s		$(OC(O)NPh)$
	122.53	s		
	127.82			
	157.85	d	3.9	
	167.65	s		$(OC(O)NPh)$
cis-$(PMe_3)_4Ru(H)(OC(O)Ph)$ (11)[e]	22.77	dd	25.3	*cis*-PMe_3
	26.27	dq	27, 3	*cis*-PMe_3
	23.12	td	14, 3	*trans*-PMe_3
	127.67	s		$(OC(O)Ph)$
	129.19	s		
	130.21	s		
	139.87	s		
	172.19	s		$(OC(O)Ph)$
cis-$(DMPE)_2Ru(Me)_2$[e]	−8.03	dq	63.3, 11.6	RuMe
	9.02	t	1.8	$Me_2PCH_2CH_2PMe_2$
	15.46	dd	10.6, 7.0	
	19.20	pent	4.5	
	22.71	dd	8.9, 5.6	
	29.20	m		$Me_2PCH_3CH_2PMe_2$
	33.57	m		
cis-$(DMPE)_2Ru(OC_6H_4$-*p*-$Me)_2$ (12)[d]	11.91	t	12.1	$Me_2PCH_2CH_2PMe_2$
	15.56	t	12.0	
	16.25	dd	15.2, 12.3	
	20.26	dd	14.4, 11.6	
	20.89	s		$(OC_6H_4$-*p*-$Me)$
	29.99	m		$Me_2PCH_3CH_2PMe_2$
	32.17	m		
	119.07	s		$(OC_6H_4$-*p*-$Me)$
	121.56	s		$(OC_6H_4$-*p*-$Me)$
	129.01	s		$(OC_6H_4$-*p*-$Me)$
	172.66	t	2.8	$(OC_6H_4$-*p*-$Me)$
$(DMPE)_2Ru(CO_3)$ (13)[h]	8.39	t	12.0	$Me_2PCH_2CH_2PMe_2$
	16.04	t	12.0	

Table IX (Continued)

compound	δ, ppm	mult[a]	*J*, Hz	assignment[b]
$(DMPE)_2Ru(CO_3)$ (**13**)[h]	16.35	t	12.0	
	18.77	t	13.6	
	26.37	m		$Me_2PCH_2CH_2PMe_2$
	33.25	m		
	167.46	s		$RuCO_3$
cis-$(DMPE)_2Ru(OC(O)Ph)_2$[h]	13.26	t	13.9	$Me_2PCH_2CH_2PMe_2$
	15.74	t	12.6	
	17.79	t	13.5	
	18.84	t	15.1	
	27.45	m		$Me_2PCH_2CH_2PMe_2$
	33.39	m		
	127.62	s		(OC(O)*Ph*)
	129.30	s		
	129.55	s		
	139.26	s		
	172.04	s		(*OC*(O)Ph)
trans-$(DMPE)_2Ru(H)(OC(O)Ph)$ (**14**)[e]	15.64	pent	5.2	$Me_2PCH_2CH_2PMe_2$
	22.49	pent	7.0	
	31.24	pent		$Me_2PCH_2CH_2PMe_2$
	127.55	s		(OC(O)*Ph*)
	128.82	s		
	129.92	s		
	139.97	s		
	170.42	s		(*OC*(O)Ph)
$(PMe_3)_3Ru(CH(C(O)CH_2CMe_3)_2)(Me)$ (**16**)[e]	4.83	dt	81.2, 11.6	RuMe
	19.01	d	13.9	PMe_3
	19.93	t	12.5	PMe_3
	30.93	s		$(CH(C(O)CH_2CMe_3)_2)$
	32.06	s		$(CH(C(O)CH_2CMe_3)_2)$
	56.53	s		$(CH(C(O)CH_2CMe_3)_2)$
	103.04	s		$(CH(C(O)CH_2CMe_3)_2)$
	128.90	s		$(CH(C(O)CH_2CMe_3)_2)$
$(PMe_3)_4Ru(OC(Me)CHC(Me)CH)$ (**19**)[e]	18.66	t	9.4	*trans*-PMe_3
	21.52	d	15.1	*cis*-PMe_3
	23.45	d	24.1	*cis*-PMe_3
	26.30	s		(OC(*Me*)CHC(*Me*)CH)
	30.50	s		(OC(*Me*)CHC(*Me*)CH)
	98.61	s		(OC(Me)*CH*C(Me)CH)
	138.18	dtd	64, 16, 10	(OC(Me)CHC(Me)*CH*)
	156.41	s		(*OC*(Me)CHC(Me)CH)
		not	observed	(*OC*(Me)CHC(Me)CH)
$(PMe_3)_4Ru(OC(O)OC(CMe_3)CH)$ (**21**)[d]	18.11	td	13.1, 2.0	*trans*-PMe_3
	21.12	d	17.2	*cis*-PMe_3
	22.58	dd	27.0, 2.2	*cis*-PMe_3
	29.53	s		(OC(O)OC(*CMe*$_3$)CH)
	38.20	d	6.0	(OC(O)OC(*C*Me$_3$)CH)
	110.98	dtd	60, 18, 8.6	(OC(O)OC(CMe$_3$)*CH*)
	151.82	d	2.8	(OC(O)OC(CMe$_3$)CH)
	156.58	t	5.3	(*OC*(O)OC(CMe$_3$)CH)

[a] The multiplicities triplet and doublet, when applied to the PMe_3 and DMPE resonances, are apparent splitting patterns. Accordingly the values reported for *J* do not necessarily reflect true coupling constants. [b] The assignment *trans*-PMe_3 refers to the mutually trans phosphine ligands; the other two phophines are assigned as *cis*-PMe_3. [c] THF-d_8, −40 °C. [d] THF-d_8, 20 °C. [e] C_6D_6, 20 °C. [f] Methanol-d_4, 20 °C. [g] CD_2Cl_2, −62 °C. [h] CD_2Cl_2, 20 °C.

Scheme XII

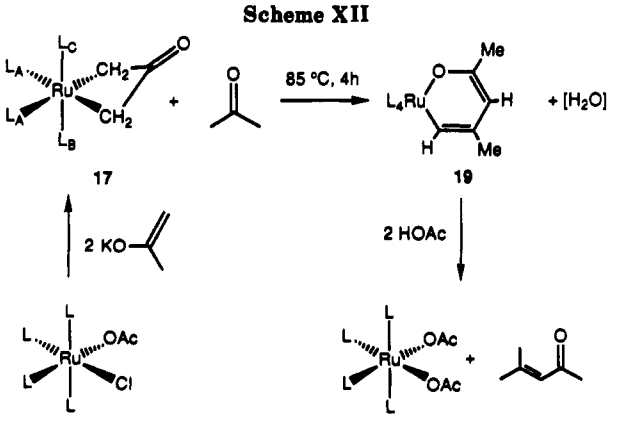

acetone to *cis*-$(PMe_3)_4Ru(OAc)(Cl)$,[19] led to clean formation of $(PMe_3)_4Ru(OC(Me)CHC(Me)CH)$ (**19**) in 45% isolated yield after heating to 85 °C for 8 h (Scheme XII).

The organic portion of **19** can be thought of as a coordinated dianion of the aldol condensation product. This complex was isolated from cold pentane as yellow crystals, which were characterized by microanalysis, as well as ^1H, $^{31}P\{^1H\}$, and $^{13}C\{^1H\}$ NMR and infrared spectroscopy. In addition, the identity of the organic ligand was confirmed by treating **19** with 2 equiv of acetic acid to form $(PMe_3)_4Ru(OAc)_2$ and free mesityl oxide in 74% yield. This free aldol product was identified by comparison of its ^1H NMR spectrum and GC retention time to those of an authentic sample. The coordinated organic fragment was identified by a doublet of doublet of triplets pattern in the ^1H and $^{13}C\{^1H\}$ NMR spectra corresponding to one metal-bound methine group and a singlet resonance corresponding to the other. Two resonances for methyl groups not bound to ruthenium were also observed in the ^1H and $^{13}C\{^1H\}$ NMR spectrum. All $^{13}C\{^1H\}$ NMR assignments were confirmed by using a DEPT pulse sequence. The A_2BC pattern in the $^{31}P\{^1H\}$ NMR spectrum, with P_B

Table X. $^{31}P\{^1H\}$ NMR Spectroscopic Data

compound	spin system[a]	δ, ppm	J, Hz
$(PMe_3)_4Ru(OC(CH_2)C_6H_4)$ (3)[d]	A_2BC	δA = 0.69	J_{AB} = 25.3
		δB = −13.71	J_{AC} = 32.2
		δC = 6.86	J_{BC} = 14.3
$(CO)(PMe_3)_3Ru(OC(Me)(Ph)CH_2C(O))$ (6)[c,e]	ABC	δA = −0.76	J_{AB} = 26.9
		δB = 8.70	J_{AC} = 26.3
		δC = 11.26	J_{BC} = 321.1
cis-$(PMe_3)_4Ru(OC_6H_4$-*p*-$Me)_2$[e] (7)	A_2B_2	δA = 14.89	J_{AB} = 31.8
		δB = −0.98	
$(PMe_3)_4Ru(CO_3)$ (8)[f]	A_2B_2	δA = 23.08	J_{AB} = 30.7
		δB = 4.75	
$(PMe_3)_4Ru(OC(NPh)O)$ (9)[g]	A_2BC	δA = 1.98	J_{AB} = 31.1
		δB = 18.96	J_{AC} = 32.8
		δC = 19.81	J_{BC} = 32.3
$(PMe_3)_4Ru(OC(O)NPh)$ (10)[h]	A_2BC	δA = 0.04	J_{AB} = 30.6
		δB = 5.66	J_{AC} = 30.6
		δC = 8.99	J_{BC} = 29.8
cis-$(PMe_3)_4Ru(H)(OC(O)$-Ph) (11)[e]	A_2BC	δA = −0.52	J_{AB} = 33
		δB = 6.74	J_{AC} = 23
		δC = −13.72	J_{BC} = 17
cis-$(DMPE)_2Ru(Me)_2$[e]	AA′BB′	δA = 45.31	$J_{AB,AB'}$ = 19.1
		δB = 32.69	
cis-$(DMPE)_2Ru(OC_6H_4$-*p*-$Me)_2$ (12)[d]	AA′BB′	δA = 52.28	$J_{AB,AB'}$ = 17.3
		δB = 36.60	
$(DMPE)_2Ru(CO_3)$ (13)[h]	AA′BB′	δA = 67.45	$J_{AB,AB}$ = 20.6
		δB = 54.86	
cis-$(DMPE)_2Ru(OC(O)Ph)_2$[h]	AA′BB′	δA = 53.99	$J_{AB,AB'}$ = 24.4
		δB = 37.44	
trans-$(DMPE)_2Ru(H)(OC$-(O)Ph) (11)[e]	A_4	δA = 46.90	
$(PMe_3)_3Ru(CH(C(O)CH_2$-$CMe_3)_2)(Me)$ (16)[e]	A_2B	δA = 25.43	J_{AB} = 16.2
		δB = −8.51	
$(PMe_3)_4Ru(OC(Me)CHC$-(Me)CH) (19)[e]	A_2BC	δ_A = −0.35	J_{AB} = 35.3
		δB = 11.85	J_{AC} = 21.8
		δC = −15.13	J_{BC} = 13.7
$(PMe_3)_4Ru(OC(O)OC$-$(CMe_3)CH)$ (21)[d]	A_2BC	δA = 0.77	J_{AB} = 36.8
		δB = 16.49	J_{AC} = 23.4
		δC = −13.21	J_{BC} = 17.9

[a] The true spin system for the *cis*-$(DMPE)_2Ru(X)_2$ compounds in this study is AA′BB′. However, all spectra of these compounds were observed simply as a pair of triplets. [b] THF-d_8, −40 °C. [c] Values for δ and J were determined by spectral simulation. [d] THF-d_8, 20 °C. [e] C_6D_6, 20 °C. [f] Methanol-d_4, 20 °C. [g] CD_2Cl_2, −62 °C. [h] CD_2Cl_2, 20 °C.

resonating upfield and P_C resonating downfield of P_A, was consistent with the presence of one ruthenium–carbon and one ruthenium–oxygen bond.

Reactions of $(PMe_3)_4Ru(\eta^2$-OC(*t*-Bu)CH) (20). Oxametallacyclobutene complex **20** was obtained by extrusion of methane from the methyl enolate complex $(PMe_3)_4Ru(Me)(OC(CH_2)CMe_3)$ at 65 °C over the course of 8 h, as described in the previous paper. Initial reactivity studies with **20** were directed toward determining if addition of protic acids and electrophiles would result in the elimination of *tert*-butylacetylene, in analogy to the behavior of **1** and **2**, or if the organic substituent would remain intact, as it did with complex **15**. The reactions of oxametallacyclobutene **20** with *p*-cresol and CO_2 are shown in Scheme XIII. Compound **20** was converted to free pinacolone (3,3-dimethyl-2-butanone) in quantitative yield by ^1H NMR spectroscopy and the bis(cresolate) complex **7** (91%) when treated with *p*-cresol. Again, the identification of the ketone was confirmed by comparison of GC retention times and ^1H NMR spectra with those of an authentic sample.

Addition of 1 equiv of CO_2 to a benzene solution of **20** led rapidly to $(PMe_3)_4Ru(\eta^2$-OC(O)OC(*t*-Bu)CH) (**21**), the product of insertion into the metal–oxygen bond. No evidence for formation of *tert*-butylacetylene was observed. Compound **21** was isolated from the reaction mixture as clear crystals in 42% yield and was characterized by ^1H, $^{31}P\{^1H\}$, and $^{13}C\{^1H\}$ NMR and infrared spectroscopy, as well as microanalysis. The inserted CO_2 moiety was identified by its $^{13}C\{^1H\}$ NMR resonance at δ 156.6 and an infrared absorption at 1633 cm^{-1}. Conclusive evidence for the presence of a ruthenium–carbon bond in the product was provided by its ^1H NMR spectrum, which contained a doublet of triplets resonance for the methine proton at δ 5.34, and by its $^{13}C\{^1H\}$ NMR spectrum, which contained a doublet of triplets of doublets resonance at δ 111.0 for the methine carbon. An A_2BC pattern in the $^{31}P\{^1H\}$ NMR spectrum, with P_B resonating upfield and P_C resonating downfield of the mutually trans phosphines, was consistent with the presence of one ruthenium–carbon and one ruthenium–oxygen bond.

Scheme XIII

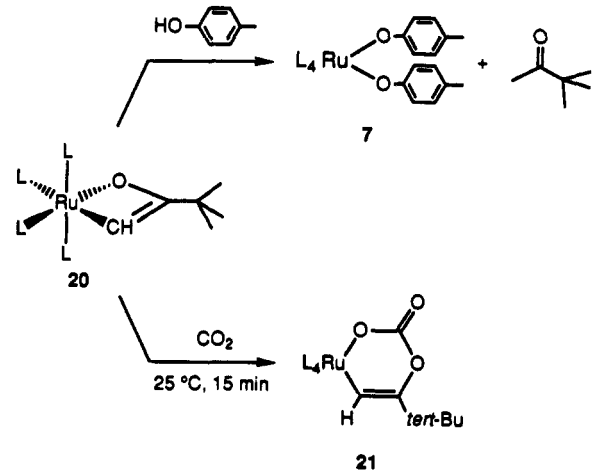

Scheme XIV

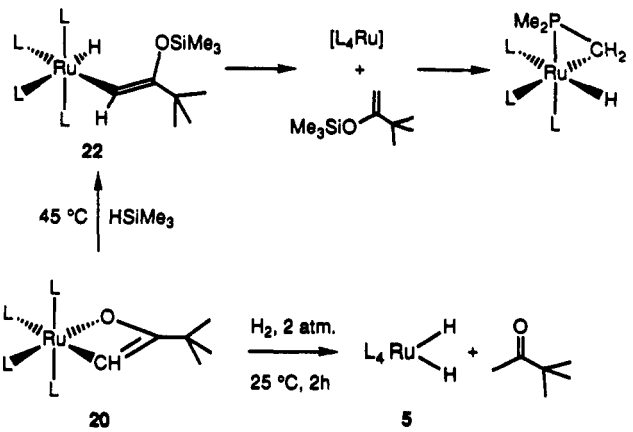

Reactions of **20** with hydrogen and trimethylsilane are shown in Scheme XIV. When a C_6D_6 solution of **20** was exposed to 2 atm of H_2, formation of free pinacolone in 61% yield by ^1H NMR spectroscopy and dihydride **5**[18,19] (77%) was observed after 1 h. Similarly, addition of trimethylsilane, followed by heating at 85 °C for 2 h, led to the silyl enol ether of pinacolone in 43% yield as the organic product. In this case, the organometallic product was the previously reported phosphine–cyclometalated complex $(PMe_3)_3Ru(CH_2PMe_2)(H)$[28,29] in 40% yield. ^1H NMR spectroscopic identification of both the ketone and silyl enol ether was confirmed by matching GC retention times to those of authentic samples.

A possible mechanism for this reaction is shown in Scheme XIV. When a solution of **20** and trimethylsilane was heated to 45 °C, an intermediate was observed by ^1H and $^{31}P\{^1H\}$ NMR spectroscopy but not fully characterized. This intermediate may be the vinyl hydride complex **22**, since formation of cyclometalated compound $(PMe_3)_3Ru(CH_2PMe_2)(H)$ as the organometallic product is consistent

(28) Werner, H.; Werner, R. *J. Organomet. Chem.* **1981**, *97*, 3272.

Scheme XV

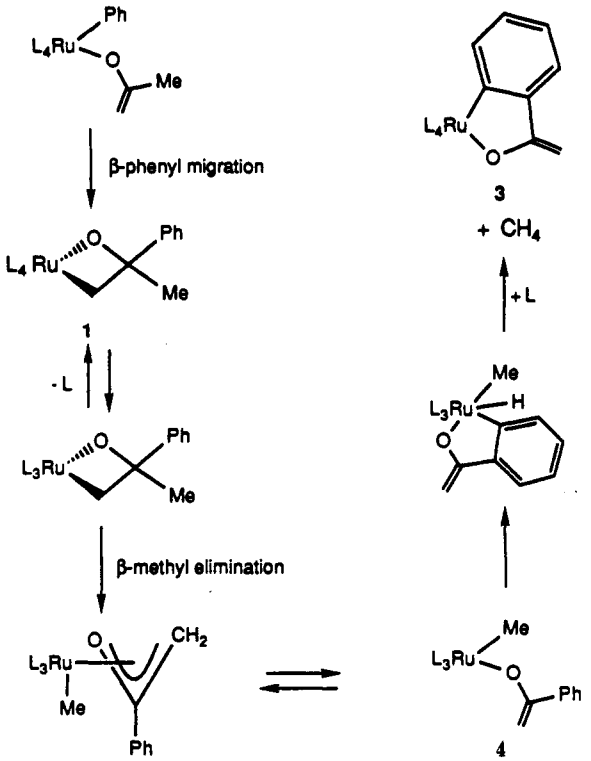

with C–H reductive elimination from 17 to form the silyl enol ether and intermediate $(PMe_3)_4Ru$. This Ru(0) intermediate was shown to form 18 cleanly in a separate study.[29]

Discussion

Effect of Dative Ligands on Reactivity. (a) Thermal Reactions. The propensity of PMe_3-substituted oxametallacycle 1 to extrude methane and form 3 at 45 °C, compared to the stability of its DMPE-substituted analogue 2 at 140 °C, is consistent with a pathway for this process that is based on the mechanism for the formation of 1 reported in the accompanying paper. A complete mechanism for the C–C cleavage process (including the preparation of metallacycle 1) is shown in Scheme XV. The mechanism involves β-Me elimination to form $(PMe_3)_4Ru(Me)(OC(CH_2)Ph)$ (4), a process that is the reverse of the phenyl migration step to form 1. Intermediate 4 simply forms methane and 3 by metalation of the aryl ring.[15,30] The experiments reported in the previous paper in this issue demonstrate that the phenyl migration step proceeds by an initial, reversible dissociation of phosphine to form an η^3-bound enolate substituent. The phenyl group then migrates to the central carbon of this η^3-bound acetone enolate. We therefore propose an analogous β-methyl elimination process to form 4 by way of an η^3-bound acetophenone enolate. Our results with the DMPE analogues are consistent with this hypothesis since the DMPE intermediate that is analogous to 4 is less likely to undergo phosphine dissociation, resulting in the stability of metallacycle 2. Although we have not obtained any mechanistic data regarding the carbonyl–methyl C–C bond cleavage reaction of 4,4-dimethyl-2-pentanone by 15, it is possible that β-methyl elimination from an oxametallacylobutane complex or another oxametallacycle is

(29) Hartwig, J. F.; Bergman, R. G.; Andersen, R. A. *J. Am. Chem. Soc.*, in press.

(30) Ryabov, A. D. *Chem. Rev.* **1990**, *90*, 403.

Scheme XVI

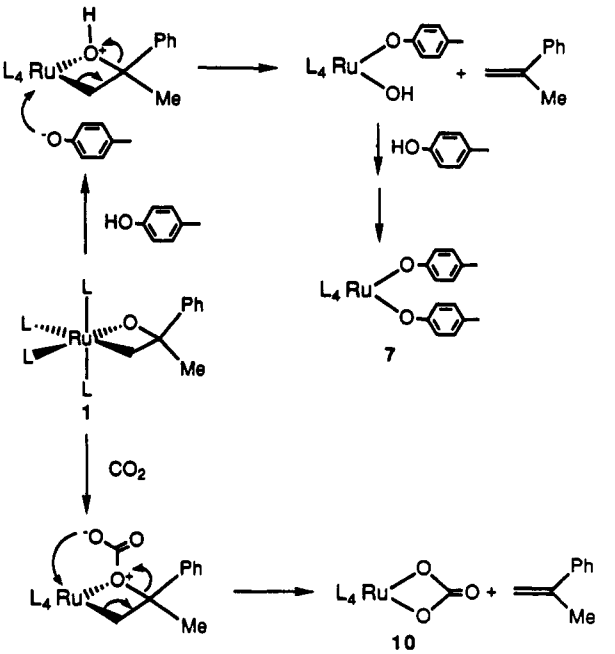

involved in this reaction. Previous examples of β-methyl elimination reactions have been reported with electrophilic early-transition-metal and lanthanide complexes,[16f,g] and a β-cyano elimination was reported to occur from a platinum oxametallacyclobutane.[6b]

(b) Reactions with Electrophiles and Protic Acids. The reactions of oxametallacycles 1 and 2 with the protic acid *p*-cresol and the electrophile CO_2 both occur at room temperature over several minutes. Because dissociation of phosphine would be expected to require higher temperatures for the DMPE complex 2 than for the PMe_3 complex 1, we conclude that reactions with these reagents occur directly at the oxygen atom of the metallacycle and do not involve coordination to the metal center by either the organic substrate or the extruded alkene, as shown in Scheme XVI. The oxygen atom connected to the electron-rich metal center is apparently basic enough to deprotonate *p*-cresol and nucleophilic enough to attack CO_2. Formation of a formal positive charge at the metallacyclic oxygen atom, followed by cleavage of the C–O bond, extrudes alkene. This process is similar to the dehydration of tertiary alcohols catalyzed by protic and Lewis acids.[31] In contrast, the reaction of these two compounds with benzaldehyde under very different conditions may reflect the involvement of phosphine dissociation during this transformation. At 110 °C it is possible that dissociation of one end of the DMPE ligand may allow coordination of the aldehyde. However, no experiments that would address the requirements for ligand dissociation in this reaction were conducted with either complex.

The failure of the oxametallacycles to incorporate alkenes or alkynes suggests that the reactions of these compounds do *not* occur by way of a ruthenium–oxo intermediate. Our results do not rigorously rule out reversible formation of a ruthenium–oxo intermediate with alkene coordinated to the metal center, but it seems likely that

(31) March, J. *Advanced Organic Chemistry*; John Wiley and Sons: New York, 1985. A referee has suggested that H_2O possibly present in our CO_2 may cause the apparent insertion reaction to proceed via a hydroxoruthenium intermediate. We cannot rule this out but feel that the fact that an analogous product (Scheme V) is formed in the reaction of 1 with PhNCO (which was carefully dried and distilled) justifies the postulation of similar mechanisms for the two processes.

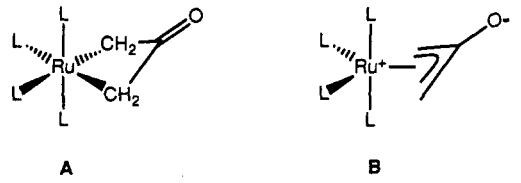

A B

Figure 5. Possible bonding modes for 17.

the resulting coordinated α-methylstyrene would dissociate at 135 °C and lead to incorporation of another alkene or alkyne into the metallacycle.

Effect of Metallacycle on Reactivity. In contrast to extrusion of alkene from 1 and 2, metallacyclobutane 17 and metallacyclobutene 20 extrude free ketone upon addition of protic acids. We propose that the aryl group of metallacycles 1 and 2 helps to stabilize the partial positive charge on the β-carbon of the metallacyle that occurs after addition of the acid or electrophile, as shown in Scheme XVI. Again, our explanation is analogous to the one used to explain the rate enhancement of ionization caused by phenyl substitution in benzyl alcohols.[31]

Effect of Ring Substitution on Structure. The *tert*-butyl substituent in compound 15 leads to a markedly different solid-state structure relative to 17, as determined by an X-ray diffraction study. First, the enolate dianion in 17 is bound through two Ru–CH_2 linkages, while the organic portion of 15 is bound by one Ru–CH_2 and one Ru–O linkage. The substitution of a bulky group in the methylene position of 17 appears to cause the *tert*-butyl-substituted cyclic enolate 15 to bind through one methylene and one oxygen atom rather than to bind through two methylene groups as was observed in 15.

The two different binding modes apparently give rise to a second dramatic difference between the two structures: the dihedral angle of 15 is 1.9°, while that in 17 is 45.6°. The solid-state structure demonstrates that the *tert*-butyl substitution does not significantly affect the steric interactions of the metallacycle with the phosphine ligands. In fact, the shortest distance between the *tert*-butyl group in 15 and the nearest phosphine methyl is greater than 1 Å longer than the shortest distance between the carbonyl oxygen atom of 17 and the nearest phosphine methyl group. The $^{31}P\{^1H\}$ NMR spectroscopic data indicate that the solution structures are similar to those in the crystalline state. Ring inversion in 17 is slow on the NMR time scale at −70 °C, as indicated by the inequivalent trans phosphine resonances observed at this temperature. The mutually trans phosphines in 15 are equivalent down to −90 °C, consistent with a nearly flat ring system or one with a dramatically lower barrier to inversion in solution.

It seems reasonable to attribute the difference in dihedral angles to electronic differences within the two rings rather than to steric or solid-state effects. Theoretical studies have indicated that the large dihedral angles in platinum metallacyclobutan-3-ones are due to a significant contribution of the bonding description **B** shown in Figure 5, and our data are consistent with this proposal.[32e] The C=O bond is significantly longer and the C(O)—C bonds are significantly shorter than those in simple organic ketones,[26] including cyclobutanones. In addition the C=O bond in 17 absorbs at 1544 cm^{-1} (data provided in companion paper), significantly lower in energy than observed for organic ketones. In contrast, the metallacycle portion of 15 contains C—C and C—O bond distances, which are similar to those observed for the enol form of organic ketones;[26] these indicate little interaction between the π-system of the ring and the ruthenium metal center.

There are few other structural data relating to the conformation of metallacyclobutane rings. Although several structurally characterized metallacyclobutan-3-ones have been reported, all of these are bound to the metal center through the two enolate carbon atoms; compound 15 is the only structurally characterized example of the alternative O- and C-bound isomer.[32] Furthermore, structural data on titanocene complexes show a trend opposite to that observed with these ruthenium complexes: X-ray structural data for titanocyclobutanes (two Ti–CH_2 linkages) show flat metallacycles,[33] while NMR spectroscopic data on titanaoxacyclobutanes analogous to compound 15 (one Ti–CH_2 linkage and one Ti–O linkage) indicate a puckered ring structure.[8a] In contrast, the structures of a platinum[6a] and a rhodium[7] oxametallacyclobutane display rings that are nearly flat. In addition, the organic analogues display the same trend; cyclobutane is bent, while oxetane is planar in the gas phase.[34]

The overall structural features of the oxatrimethylenemethane complex 18 are similar to those observed with parent trimethylenemethane complexes.[35] Principally, the central carbon atom of the organic ligand is located significantly out of the plane of the other three atoms. This similarity contrasts with observations made on other recently reported heteroatom-substituted systems. In particular, an oxatrimethylenemethane complex of $Fe(CO)_3$ adopts a dimeric structure,[36] and a thiatrimethylenemethane complex of $Fe(CO_3)$[37] shows an unsymmetrically bound organic ligand, perhaps due to phenyl substitution at one carbon and *tert*-butyl substitution at the other. A nearly planar oxatrimethylenemethane fragment was observed in a dimeric ruthenium complex.[38] The central carbon was only 0.07 Å above the plane of the other three atoms.

Insertion Reactions with CO and CO_2. Extensive mechanistic information indicates that insertion of CO into metal–alkyl bonds involves coordination of free carbon monoxide to the metal center, followed by migration of the alkyl group.[39] Therefore, it is not surprising that the DMPE-substituted metallacycle 3 is inert toward insertion of CO into the metal–carbon bond, while PMe_3-substituted metallacycle 1 readily reacts with CO to form insertion product 6. However, it is interesting to note that CO reacts

(32) (a) Clarke, D. A.; Kemmitt, R. D. W.; Mazid, M. A.; McKenna, P.; Russell, D. R.; Schilling, M. D.; Sherry, L. J. S. *J. Chem. Soc., Dalton Trans.* **1984**, 1993. (b) Kemmitt, R. D. W.; McKenna, P.; Russell, D. R.; Sherry, L. J. S. *J. Chem. Soc., Dalton Trans.* **1985**, 259. (c) Imram, A.; Kemmitt, R. D. W.; Markwick, A. J. W.; McKenna, P.; Russell, D. R.; Sherry, L. J. S. *J. Chem. Soc., Dalton Trans.* **1985**, 549. (d) Jones, M. D.; Kemmitt, R. D. W.; Fawcett, J.; Russell, D. R. *J. Chem. Soc., Chem. Commun.* **1986**, 427. (e) Fawcett, J.; Henderson, W.; Jones, M. D.; Kemmitt, R. D. W.; Russell, D. R.; Lam, B.; Kang, S. D.; Albright, T. A. *Organometallics* **1989**, *8*, 1991.

(33) Lee, J. B.; Gajda, G. J.; Schaefer, W. P.; Howard, T. R.; Ikariya, T.; Straus, D. A.; Grubbs, R. H. *J. Am. Chem. Soc.* **1981**, *103*, 7358.

(34) (a) Legon, A. C. *Chem. Rev.* **1980**, *80*, 231. (b) Chan, S. I.; Zinn, J.; Gwinn, W. D *J. Chem. Phys.* **1961**, *34*, 1319.

(35) (a) Grosselin, J.-M.; Le Bozec, H.; Moinet, C. Toupet, L.; Köhler, F. H.; Dixneug, P. H. *Organometallics* **1988**, *7*, 88. (b) Jones, M. D.; Kemmitt, R. D. W.; Platt, A. W. G. *J. Chem. Soc., Dalton Trans.* **1986**, 1411. (c) Allen, S. R.; Barnes, S. G.; Green, M.; Moran, G.; Trollope, L.; Murrall, N. W.; Welch, A. J.; Sharaiba, D. M. *J. Chem. Soc., Dalton Trans.* **1984**, 1157.

(36) Frey, M.; Jenny, T. A.; Stoeckli-Evans, H. *Organometallics* **1990**, *9*, 1806.

(37) Ando, W.; Choi, N.; Kabe, Y. *J. Am. Chem. Soc.* **1990**, *112*, 4574.

(38) Holmgren, J. S.; Shapley, J. R.; Wilson, S. R.; Pennington, W. T. *J. Am. Chem. Soc.* **1986**, *108*, 508.

(39) (a) Alexander, J. J. *The Chemistry of the Metal-Carbon Bond*; Hartley, F. R., Ed.; Wiley: New York, 1985; Vol. 2, Chapter 5. (b) Yamamoto, A. *Organotransition Metal Chemistry*; Wiley: New York, 1986. (c) Collman, J. P.; Hegedus, L. S.; Norton, J. R.; Finke, R. G. *Principles and Applications of Organotransition Metal Chemistry*; University Science Books: Mill Valley, CA, 1987; p 356.

with the Ru–C bond of 1 in preference to the Ru–O bond and that metallacycle 2 is inert toward insertion of CO into the metal–oxygen bond. This demonstrates that migration of the methylene end of the metallacycle is faster than migation of the alkoxide end. Moreover, a mechanism involving direct insertion of CO into the metal–heteroatom bond or dissociation of an alkoxide anion followed by attack of a coordinated or free CO does not occur in this ruthenium system. Such a mechanism has been reported to occur with a square-planar iridium system,[40] but intramolecular migration to a coordinated ligand appears to occur with other systems.[41]

In contrast to the alkene extrusion processes that occur upon addition of CO_2 to oxametallacyclobutanes 1 and 2, as well as the propensity of 1 to undergo insertion of CO into the metal–carbon bond, addition of CO_2 to oxametallacyclobutene 20 led to insertion into the ruthenium–oxygen bond. An extensive report of relative insertion rates of CO and CO_2 with other compounds of the $(PMe_3)_4Ru(X)(Y)$ system is provided in a separate study,[42] including the insertion of CO_2 into the metal–carbon bond of the cyclometalated $(PMe_3)_4Ru(OC_6H_3Me)$ (23).

The results in that study suggested that selectivities were controlled by the nucleophilicity of the heteroatom of the metallacycle and electrophilicity of the organic substrate. In light of these earlier results, we propose that the greater nucleophilicity of the enolate oxygen atom of 20 (compared to the aryl oxide oxygen atom of 23) and the greater electrophilicity of CO_2 (compared to CO) allows for direct attack of CO_2 by the oxygen atom of 20. Such a mechanism would account for the observed selectivities of compounds 1, 20, and 23 for CO and CO_2.

Experimental Section

General. Unless otherwise noted, all manipulations were carried out under an inert atmosphere in a Vacuum Atmospheres 553-2 drybox with an attached M6-40-1H Dritrain or by using standard Schlenk or vacuum line techniques. Information on methods for solvent purification and for obtaining spectroscopic data is provided in the companion paper.

Unless otherwise specified, all reagents were purchased from commercial suppliers and used without further purification. PMe_3 (Strem) was dried over NaK or a Na mirror and vacuum transferred prior to use. DMPE (1,2-bis(dimethylphosphino)ethane) (Strem) was used as received. Ferrocene (Aldrich) was sublimed, and mesitylene was dried over sodium/benzophenone ketyl and distilled prior to use. *p*-Cresol was dried by refluxing a solution in benzene using a Dean-Stark trap followed by distillation under argon. Acetophenone and benzaldehyde were dried by refluxing over CaH_2, followed by distillation under nitrogen. Hydrogen, carbon monoxide, and carbon dioxide were purchased from Matheson and used as received. Trimethylsilane was purchased from Petrarch and used as received. 4,4-Dimethyl-2-pentanone and pinacolone were purchased from Aldrich and used as received. *tert*-Butylacetylacetone was prepared by the addition of the potassium enolate of 4,4-dimethyl-2-pentanone to *tert*-butylacetyl chloride. $Me_3SiOC(CH_2)CMe_3$ was prepared by standard methods.[43] Alkali enolates were prepared as described in the companion paper as was the mixture of *cis*- and *trans*-$(PMe_3)_4Ru(Ph)(Cl)$. $(PMe_3)_4Ru(\eta^2\text{-}C_6H_4)$,[15] *cis*-$(PMe_3)_4Ru(OAc)(Cl)$,[19] and *trans*-$(PMe_3)_4Ru(Cl)_2$[21] were prepared as published previously.

Pentane and hexane (UV grade, alkene free) were distilled from $LiAlH_4$ under nitrogen. Benzene, toluene, and tetrahydrofuran were distilled from sodium benzophenone ketyl under nitrogen. Dichloromethane was either distilled under N_2 or vacuum transferred from CaH_2. Deuterated solvents for use in NMR experiments were dried as their protiated analogues but were vacuum transferred from the drying agent.

$(PMe_3)_4Ru(OC(CH_2)C_6H_4)$ (3). (a) By Thermolysis of 1. In 2.4 mL of C_6D_6 was dissolved 25.0 mg (0.0483 mmol) of *cis*- and *trans*-$(PMe_3)_4Ru(Ph)(Cl)$ and 5 mg of ferrocene as an internal standard. Into an NMR tube was placed 0.6 mL of this solution for determination of the relative concentrations of *cis*- and *trans*-$(PMe_3)_4Ru(Ph)(Cl)$ and the internal standard. To the remaining solution was added 10.4 mg (3.0 equiv) of $KOC(CH_2)Me$. The resulting suspension was stirred for 2 h, over which time the yellow color turned darker orange. The solid was removed by forcing the suspension through a small plug of Celite. The resulting solution containing 1 was equally divided into three separate NMR tubes, one for use in this preparation, a second for part c below, and a third for use in the preparation of 7 from 1. The first tube was equipped with a vacuum stopcock, degassed by three freeze, pump, thaw cycles, and sealed under vacuum. The sample was then heated to 45 °C for 8 h. ^1H and $^{31}P\{^1H\}$ NMR of the final reaction solution showed formation of 3 in 51% yield, as determined by comparison to the initial sample.

(b) By Addition of $KOC(CH_2)Ph$ to $(PMe_3)_4Ru(Me)(Cl)$. In 1.4 mL of C_6D_6 was dissolved 18.8 mg (0.0413 mmol) of $(PMe_3)_4Ru(Me)(Cl)$ and 1.4 mL of ferrocene as an internal standard. Half of this solution was placed into an NMR tube and to the remaining solution was added 5 mg (1.5 equiv) of $KOC(CH_2)Ph$ as a solid. The resulting suspension was stirred for 5 min at room temperature and then placed into a second NMR tube. The ^1H NMR spectrum of this solution showed the presence of 3 and starting material. No 4 was observed. The solution was allowed to stand at room temperature for 24 h, after which time the ^1H NMR spectrum showed the presence of methane and the formation of 3 in 98% yield, by comparison with the sample of *cis*- and *trans*-$(PMe_3)_4Ru(Ph)(Cl)$ and ferrocene internal standard.

(c) By Addition of Acetophenone to 1. To the second sample of 1, generated as described in part a, was added 2.4 μL (1.2 equiv) of acetophenone. The tube was equipped with a vacuum stopcock, degassed by three freeze, pump, thaw cycles, and sealed under vacuum. The sample was then heated to 45 °C for 8 h. ^1H and $^{31}P\{^1H\}$ NMR of the final reaction solution showed formation of α-methylstyrene (58%) and 3 (61%),[15] as determined by comparison to the initial sample.

Hydrogenolysis of 1. In 1.2 mL of C_6D_6 was dissolved 15.0 mg of *cis*- and *trans*-$(PMe_3)_4Ru(Ph)(Cl)$ and 2 mg of ferrocene as an internal standard. Into one NMR tube was placed half of the reaction solution and to the remaining solution was added 1.5 mg (1.0 equiv) of $KOC(CH_2)Me$ as a solid. The reaction was stirred for 4 h, after which time the orange solution was filtered through a small plug of Celite and the filtrate was placed into a 9-in. NMR tube equipped with a Kontes vacuum adaptor. The sample was degassed by three freeze, pump, thaw cycles, submerged in liquid nitrogen, and exposed to 450 torr of H_2. The tube was sealed at the top of the liquid nitrogen to give a final length of 8.5 in. and a pressure of approximately 2 atm at 25 °C. After 2 h at 25 °C, the orange solution became pale yellow, and ^1H and $^{31}P\{^1H\}$ NMR spectroscopy showed formation of the dihydride 5 in 88% yield and the alcohol $HOC(Me)_2Ph$ in 84% yield, by comparison to the sample of *cis*- and *trans*-$(PMe_3)_4Ru(Ph)(Cl)$ and ferrocene internal standard. The sample was then opened and the solution passed through a short column of silica to remove the ruthenium complex. After elution with 1 mL of ether, gas chromatographic analysis of the eluent showed the 2-phenyl-2-propanol as the major peak after those of the solvent, as determined by comparison of the retention time to an authentic sample and coinjection of the eluent and a solution of the authentic sample.

$(PMe_3)_3(CO)Ru(OC(Me)(Ph)CH_2C(O))$ (6). To a suspension of 150 mg of *cis*- and *trans*-$(PMe_3)_4Ru(Ph)(Cl)$ in 14 mL of *n*-pentane was added at room temperature 83.5 mg (3.0 equiv) of $KOC(CH_2)Me$ as a solid. The suspension was stirred for 4 h, and after this time the solid was removed by filtration with pressure through a plug of Celite. The resulting clear orange filtrate was transferred to a 250-mL glass reaction vessel equipped with a Kontes vacuum adaptor. The vessel was submerged in liquid

(40) Rees, W. M.; Atwood, J. D. *Organometallics* **1985**, *4*, 402.
(41) (a) Bryndza, H. E. *Organometallics* **1985**, *4*, 406. (b) Bryndza, H. E.; Fultz, W. C.; Tam, W. *Organometallics* **1985**, *4*, 939. (c) Bryndza, H. E. *Organometallics* **1985**, *4*, 1687. (d) Cowan, R. L.; Trogler, W. C. *J. Am. Chem. Soc.* **1989**, *111*, 4750. (e) Glueck, D. S.; Newman Winslow, L. J.; Bergman, R. G. *Organometallics* **1991**, *10*, 1462.
(42) Hartwig, J. F.; Andersen, R. A.; Bergman, R. A. *J. Am. Chem. Soc.*, in press.
(43) Miller, R. D.; McKean, D. R. *Synthesis* **1979**, 730.

nitrogen and exposed to vacuum followed by 450 torr of CO. Upon thawing, the yellow solution became clear. The volume was reduced to ~6 mL and cooled to −40 °C to provide 76.0 mg (50.1%) of white needles. IR (KBr) 1907 (s), 1614 (s); MS (FAB, sulfolane) 520 (M^+). Anal. Calcd for $C_{20}H_{37}O_3P_3Ru$: C, 46.23; H, 7.18. Found: C, 46.00; H, 7.38.

Reaction of 1 with *p*-Cresol. A solution of 5 mg (4 equiv) of *p*-cresol in 0.3 mL of C_6D_6 was prepared. The third sample of **1**, prepared as described in the section on the formation of **3** by thermolysis of **1**, was treated with the solution of *p*-cresol dropwise until the dark orange solution turned yellow (approximately 0.2 mL of the solution). ^1H and $^{31}P\{^1H\}$ NMR of the resulting solution showed formation of α-methylstyrene in 86% yield and **7**[20] in 74% yield, by comparison to the sample of *cis*- and *trans*-$(PMe_3)_4Ru(Ph)(Cl)$ and ferrocene internal standard.

$(PMe_3)_4Ru(CO_3)$ (8). (a) From 1. In 1.8 mL of C_6D_6 was dissolved 14.4 mg (0.0278 mmol) of *cis*- and *trans*-$(PMe_3)_4Ru(Ph)(Cl)$ and 3 mg of ferrocene as an internal standard. Into an NMR tube was placed 0.6 mL of this solution for an integration of starting material versus the internal standard. To the remaining solution was added 3.5 mg (1.3 equiv) of $KOC(CH_2)Me$. The resulting suspension was stirred for 2 h, over which time the yellow color turned darker orange. The resulting solution containing **1** was divided equally into two NMR tubes. One of the tubes was equipped with a vacuum stopcock and degassed by three freeze, pump, thaw cycles. To this sample was added 0.0556 mmol of CO_2 by vacuum transfer. Upon thawing, the orange solution turned clear and white crystals formed from the reaction solution. ^1H NMR spectroscopy of this solution showed the presence of α-methylstyrene in 84% yield. The tube was then opened and CD_2Cl_2 (0.2 mL) was added to dissolve the ruthenium complex. ^1H and $^{31}P\{^1H\}$ NMR spectroscopy showed the formation of **8** in 83% yield, by comparison to the sample of *cis*- and *trans*-$(PMe_3)_4Ru(Ph)(Cl)$ and ferrocene internal standard.

(b) Preparative Scale. Into a 50-mL round-bottom flask equipped with a Kontes vacuum adaptor was placed, in air, 300 mg (0.630 mmol) of *trans*-$(PMe_3)_4Ru(Cl)_2$ and 150 mg (1.09 mmol) of K_2CO_3. To these two solids was added 10 mL of methanol. The resulting solution was carefully degassed by three freeze, pump, thaw cycles and then heated at 50 °C for 1.5 h with stirring. During this time, the initial orange solution turned pale yellow. The solvent was removed under reduced pressure and the resulting solid was extracted with CH_2Cl_2. Removal of the CH_2Cl_2 solvent provided 255 mg (85%) of white solid, which was pure by $^{31}P\{^1H\}$ NMR spectroscopy. This material was further purified by dissolving the material in CH_2Cl_2 and layering the resulting solution with Et_2O to provide 10.6 mg (3.5%) of white powder, used for infrared and mass spectral analysis. IR (KBr) 1578 (s); MS (FAB, 1,2-dinitrobenzyl alcohol matrix) 467 (MH^+), 423 ($(M - CO_2)H^+$), 407 ($(M - CO_3)H^+$), 391 ($(M - PMe_3)H^+$).

Synthesis of $(PMe_3)_4Ru(OC(O)NPh)$ (10) via $(PMe_3)_4Ru(OC(NPh)O)$ (9). In 10 mL of *n*-pentane was suspended 301 mg of *cis*- and *trans*-$(PMe_3)_4Ru(Ph)(Cl)$ and 120 mg (1.98 equiv) of $KOC(CH_2)Me$. The reaction was stirred for 4 h at room temperature, after which time the orange suspension was filtered with pressure. To the resulting clear orange solution was added 95.0 mg of PhNCO (1.98 equiv) as a solution in 1 mL of *n*-pentane. Upon addition of the isocyanate, a pale yellow solid precipitated from solution. This solid was filtered, washed twice with 1.5 mL of *n*-pentane, and dried under vacuum to provide a 194-mg (63%) yield of **9**, which was roughly 90% pure by ^1H and $^{31}P\{^1H\}$ NMR spectroscopy. This material was dissolved in 7 mL of CH_2Cl_2 and heated to 45 °C for 1 h to convert **9** to its isomer **10**. The solution was concentrated to 1 mL under reduced pressure and layered with 4 mL of pentane. After 12 h at room temperature, 52.6 mg (27.1%) of analytically pure yellow powder was collected. IR (KBr) 2912 (m), 1595 (s), 1577 (m), 1567 (m), 1550 (m), 1492 (m), 1482 (m), 1329 (s), 1314 (m), 1304 (m), 1282 (m), 1233 (m), 944 (s). Anal. Calcd for $C_{19}H_{41}NO_2P_4Ru$: C, 42.22; H, 7.65; N, 2.59. Found: C, 42.45; H, 7.67; N, 2.49.

$(PMe_3)_4Ru(H)(OC(O)Ph)$ (11). (a) From 1. In 1.2 mL of C_6D_6 was dissolved 10.8 mg (0.0209 mmol) of *cis*- and *trans*-$(PMe_3)_4Ru(Ph)(Cl)$ and 2 mg of ferrocene as an internal standard. Half of this solution was transferred to an NMR tube, and to the remaining solution was added 3 mg (1.5 equiv) of $KOC(CH_2)Me$ as a solid. The reaction was stirred for 2 h, after which time the solid materials were removed by filtration through a small plug of Celite. Benzaldehyde (2.1 μL, 1.0 equiv) was added dropwise at room temperature as a solution in 0.3 mL of C_6D_6. The resulting yellow solution was placed into an NMR tube, equipped with a Kontes vacuum adaptor, and sealed under vacuum. The sample was then heated to 45 °C for 24 h, after which time ^1H and $^{31}P\{^1H\}$ NMR spectroscopy showed formation of **11** in 53% yield and α-methylstyrene in 76% yield.

(b) Preparative Scale. In a glass reaction vessel equipped with a Kontes vacuum adaptor was placed a solution of 374 mg of $(PMe_3)_4Ru(C_2H_4)$ in 10 mL of C_6H_6. To this stirred solution was added 105 mg (1.0 equiv) of benzoic acid in 2 mL of C_6H_6. The vessel was then closed and heated to 45 °C for 24 h, after which time the solvent was removed under reduced pressure and the residue was extracted with 10 mL of pentane. Concentration of the solution and cooling to −40 °C provided 64.3 mg (14%) of analytically pure white needles. IR (KBr) 1826 (s), 1599 (s). Anal. Calcd for $C_{19}H_{42}O_2P_4Ru$: C, 43.26; H, 8.02. Found: C, 43.12; H, 8.10.

$(DMPE)_2Ru(OC_6H_4$-*p*-$Me)_2$ (12). (a) From 2. In 0.6 mL of C_6D_6 was dissolved 7.1 mg (0.0133 mmol) of **2** and 2 mg of mesitylene as an internal standard. A ^1H NMR spectrum of this solution was obtained. To this solution was then added 2.9 mg (2.0 equiv) of *p*-cresol as a solid. A second ^1H NMR and $^{31}P\{^1H\}$ NMR spectrum showed formation of α-methylstyrene in quantitative yield and **12** in 74% yield.

(b) Preparative Scale. In 5 mL of toluene was dissolved 325 mg (0.754 mmol) of *cis*-$(DMPE)_2Ru(Me)_2$. To the stirred solution was added, dropwise at room temperature, 179 mg (2.2 equiv) of *p*-cresol in 1 mL of toluene. During this addition, the initial clear solution turned yellow, and gas evolution was observed. The solution was layered with 3 mL of pentane, and after 12 h, 146 mg (32%) of **12**, judged pure by ^1H and $^{31}P\{^1H\}$ NMR spectroscopy, was isolated. This material was recrystallized for microanalysis by vapor diffusion of pentane into a solution of **12** in toluene. IR (KBr) 2995 (w), 2972 (m), 2906 (s), 2855 (w), 1601 (m), 1500 (s), 1497 (s), 1420 (m), 1304 (s), 1159 (m), 1099 (m), 929 (s). Anal. Calcd for $C_{26}H_{46}O_2P_4Ru$: C, 50.72; H, 7.53. Found: C, 50.26; H, 7.52.

$(DMPE)_2Ru(CO_3)_2$ (13). (a) From 2. In 0.6 mL of C_6D_6 was dissolved 7.1 mg (0.0133 mmol) of **2** and 2 mg of mesitylene as an internal standard. A ^1H NMR spectrum of this solution was obtained. The NMR tube was then equipped with a Kontes vacuum adaptor. To the sample was added 2.0 equiv of CO_2 by vacuum transfer. Upon thawing, **13** crystallized from the reaction mixture. A second ^1H NMR spectrum showed formation of α-methylstyrene in 96% yield. The tube was then opened and CD_2Cl_2 (~0.2 mL) was added to the solution to dissolve **13**. ^1H and $^{31}P\{^1H\}$ NMR spectroscopy of the resulting solution showed formation of **13** in quantitative yield.

(b) Preparative Scale. Into a glass reaction vessel equipped with a Kontes vacuum adaptor was placed 250 mg (0.538 mmol) of **8**, 15 mL of tetrahydrofuran, and 242 mg (3.0 equiv) of DMPE. The reaction vessel was frozen with liquid nitrogen, exposed to vacuum, closed, and heated to 85 °C for 24 h. After this time the $^{31}P\{^1H\}$ NMR spectrum of an aliquot showed complete conversion of **8** to **13**. The solvent was removed under reduced pressure and the resulting solid was washed with hexanes to provide 83.0 mg (33.5%) of white powder, which was roughly 95% pure. Attempts to obtain analytically pure material by crystallization were not successful. IR (KBr) 1566 (s).

$(DMPE)_2Ru(H)(OC(O)Ph)$ (14). (a) From 2. In 1.2 mL of C_6D_6 was dissolved 12.6 mg (0.0237 mmol) of **2** and 2 mg of mesitylene as an internal standard. Half of this solution was placed into an NMR tube, and to the remaining solution was added 1.3 μL (1.1 equiv.) of benzaldehyde. The reaction was then placed into an NMR tube equipped with a Kontes vacuum adaptor and degassed by three freeze, pump, thaw cycles. The sample was then heated at 110 °C for 2 days, and ^1H NMR spectroscopy showed formation of α-methylstyrene in quantitative yield and **14** in 57% yield.

(b) Preparative Scale. In 4 mL of hexanes was dissolved 78.4 mg of *cis*-$(DMPE)_2Ru(Me)_2$. To this solution was added 44.4 mg (2 equiv) of benzoic acid. The reaction was stirred for 24 h at room temperature, over which time the product $L_4Ru(OC(O)Ph)_2$ precipitated from the reaction as a white solid. This solid was

isolated by filtration and washed twice with 2 mL of pentane to provide 83.5 mg (71.4%) of product, which was pure enough (~90%) for preparation of 14. The bis(benzoate) (0.130 mmol) was dissolved in 7 mL of tetrahydrofuran. To the stirred solution was added dropwise at room temperature 32.5 μL (0.0325 mmol) of a 1.0 M solution of lithium aluminum hydride in Et_2O. The resulting solution was stirred for 8 h, after which time the solvent was removed under reduced pressure, and the residue was extracted three times with a total of 25 mL of Et_2O. The solution volume was reduced to ~5 mL in vacuo and cooled to −40 °C to provide 67.9 mg (53.4%) of analytically pure white needles. IR (KBr) 2964 (m), 2921 (m), 2899 (s), 1907 (m), 1601 (s), 1566 (s), 1552 (m), 1419 (m), 1396 (m), 1360 (s), 1291 (m), 1275 (m), 937 (s), 929 (s) cm^{-1}. Anal. Calcd for $C_{19}H_{38}O_2P_4Ru$: C, 43.60; H, 7.32. Found: C, 43.32; H, 7.23.

Reactions of $(PMe_3)_4Ru(OC(CHCMe_3)CH_2)$ (15). Reaction with *p*-Cresol. Into an NMR tube was placed a solution of 6.8 mg of 15, 2 mg of mesitylene as an internal standard, and 0.6 mL of C_6D_6. A ^1H NMR spectrum of this initial solution was obtained. To this sample was then added 3.2 mg of *p*-cresol as a solid. ^1H NMR spectroscopy showed quantitative formation of both 7 and 4,4-dimethyl-2-pentanone, as determined by comparison to the initial spectrum.

Reaction with 4,4-Dimethyl-2-pentanone To Form $(PMe_3)_3Ru(CH(C(O)CH_2CMe_3)_2)(Me)$ (16). (a) From 15. In 0.6 mL of C_6D_6 was dissolved 12.6 mg (0.0252 mmol) of 15 and 2 mg of mesitylene as an internal standard. To this solution was added 2.9 mg (1.0 equiv) of 4,4-dimethyl-2-pentanone, and the reaction was transferred to an NMR tube equipped with a Kontes vacuum adaptor. The sample was degassed by three freeze, pump, thaw cycles and sealed. A ^1H NMR spectrum of this initial solution was obtained. The reaction was then heated to 110 °C for 24 h, after which time ^1H and $^{31}P\{^1H\}$ NMR spectroscopy showed formation of 16 in 77% yield.

(b) Preparative Scale. Into a glass reaction vessel equipped with a Kontes vacuum adaptor was placed a solution of 146 mg (0.304 mmol) of $(PMe_3)_4Ru(\eta^2\text{-}C_6H_4)$ and 76.1 mg (2.2 equiv) of 4,4-dimethyl-2-pentanone in 7 mL of C_6H_6. The solution was heated for 24 h at 110 °C, over which time the initial clear solution turned yellow. The solvent was removed under reduced pressure and the residue extracted into 10 mL of *n*-pentane. The pentane solution was filtered through a small plug of Celite, concentrated to ~2 mL, and cooled to −40 °C to provide 59.0 mg (35%) of yellow blocks, judged pure by ^1H, $^{31}P\{^1H\}$, and $^{13}C\{^1H\}$ NMR spectroscopy. This material was then recrystallized from pentane for microanalysis. IR (KBr) 2966 (s), 2944 (s), 2906 (s), 2861 (m), 1576 (s), 1561 (w), 1514 (s), 1468 (m), 1452 (m), 1446 (m), 1434 (m), 1428 (m), 1408 (m), 1363 (m), 1293 (m), 1273 (s), 966 (s), 939 (s) cm^{-1}. Anal. Calcd for $C_{21}H_{35}O_2P_4Ru$: C, 49.72; H, 9.61. Found: C, 49.46; H, 9.64.

Addition of HCl to 16. Into an NMR tube equipped with a rubber septum was placed a solution of 5.6 mg of 16 and 2 mg of mesitylene as an internal standard in 0.6 mL of C_6D_6. A ^1H NMR spectrum of this solution was obtained. To this solution was then added 3 μL of 37% HCl in water, and immediate formation of a solid occurred. ^1H NMR spectroscopy showed formation of *tert*-butylacetylacetone in quantitative yield, as determined by comparison to the initial spectrum. The sample was then filtered to remove the insoluble ruthenium complex. Gas chromatographic analysis performed on the resulting clear filtrate showed the presence of *tert*-butylacetylacetone, as determined by comparison of the retention time to that of an authentic sample, as well as coinjection of the reaction solution with the authentic sample.

$(PMe_3)_4Ru(OC(Me)CHC(Me)CH)$ (19). A suspension of $(PMe_3)_4Ru(OAc)(Cl)$ (127 mg, 0.254 mmol) and $KOC(CH_2)Me$ (53.7 mg, 2.2 equiv) in 7 mL of ether was stirred for 2 h at room temperature. After this time, the solution was transferred to a glass reaction vessel equipped with a Kontes vacuum adaptor. The solution was frozen in liquid nitrogen and exposed to vacuum. The vessel was closed and then heated to 85 °C for 8 h. After this time, the solvent was removed and the residue was extracted into 10 mL of pentane. The resulting slurry was filtered through a small plug of Celite, concentrated to ~2 mL, and cooled to −40 °C to provide 57.7 mg (45%) of yellow crystals of roughly 95% purity by ^1H, $^{31}P\{^1H\}$, $^{13}C\{^1H\}$ NMR spectroscopy. This material was recrystallized from pentane to provide an analytically pure sample of 19. IR (KBr) 2987 (m), 2968 (s), 2967 (s), 2907 (s), 2829 (m), 1581 (s), 1528 (m), 1437 (m), 1419 (m), 1414 (m), 1394 (s), 1295 (s), 13272 (s), 1187 (s), 947 (s) cm^{-1}. Anal. Calcd for $C_{18}H_{44}OP_4Ru$: C, 43.11; H, 8.84. Found: C, 43.22; H, 8.90.

Addition of HOAc to 19. Into an NMR tube equipped with a Kontes vacuum adaptor was placed a solution of 8.6 mg of 19 and 2 mg of mesitylene in 0.6 mL of C_6D_6. A ^1H NMR spectrum of this solution was obtained to determine the relative concentrations of starting material and internal standard. Acetic acid (2.0 μL, 2.0 equiv) was then added to the sample. The solution was frozen in liquid nitrogen and exposed to vacuum. The tube was sealed and the sample was heated at 85 °C for 2 h, after which time ^1H and $^{31}P\{^1H\}$ NMR spectroscopy showed formation of $(PMe_3)_4Ru(OAc)_2$ in quantitative yield and mesityl oxide in 74% yield. The sample tube was then opened and the solution was passed through a short column of silica to remove the ruthenium complex, eluting with 1 mL of ether. Gas chromatographic analysis of the eluent showed the presence of $CH_3C(O)CH{=}CMe_2$, as determined by comparison of the retention time to an authentic sample as well as coinjection of the eluent and an authentic sample.

Reactions of $(PMe_3)_4Ru(OC(CMe_3)CH)$ (20). Reaction with *p*-Cresol. Into an NMR tube was placed a solution of 7.2 mg of 20 and 2 mg of mesitylene as an internal standard in 0.6 mL of C_6D_6. A ^1H NMR spectrum of this initial solution was obtained. To this sample was then added 3.5 mg of *p*-cresol as a solid. ^1H NMR spectroscopy showed formation of 7 in 91% yield and pinacolone (3,3-dimethyl-2-butanone) in quantitative yield, as determined by comparison to the initial spectrum.

Reaction with CO_2 To Form $(PMe_3)_4Ru(OC(O)OC(CMe_3)CH)$ (21). Into a medium-walled NMR tube was placed a solution of 41.2 mg (0.0819 mmol) of 20 in 0.4 mL of THF-d_8. The tube was equipped with a Kontes vacuum adaptor and degassed by three freeze, pump, thaw cycles. To the solution was added 0.0819 mmol of CO_2 by vacuum transfer. The tube was sealed and the initial yellow solution turned a paler yellow color upon thawing. ^1H, $^{13}C\{^1H\}$, and $^{31}P\{^1H\}$ NMR spectroscopy showed clean conversion to 21. Upon standing for 12 h, 18.9 mg (42%) of pure 21 as white blocks formed from the reaction solution. This material was recrystallized for microanalysis by diffusing pentane into a THF solution of 21. IR (KBr) 2972 (m), 2956 (m), 2944 (s), 2910 (m), 1633 (s), 1430 (m), 1325 (m), 1313 (m), 1297 (m), 1279 (m), 1042 (s), 944 (s) cm^{-1}. Anal. Calcd for $C_{19}H_{46}O_3P_4Ru$: C, 41.70; H, 8.47. Found: C, 41.32; H, 8.44.

Reaction with H_2. In 1.8 mL of C_6D_6 was dissolved 18.3 mg of 20 and 4 mg of mestiylene as an internal standard. The solution was divided into three equal portions. One portion was placed into an NMR tube to determine the relative concentrations of starting material and the internal standard. The second portion was placed into an NMR tube equipped with a Kontes vacuum adaptor. The latter sample was degassed by two freeze, pump, thaw cycles, immersed in liquid nitrogen, and exposed to 450 torr of H_2. The tube was sealed at the level of the liquid nitrogen and heated to 45 °C for 8 h to provide the dihydride 5 in 77% yield and pinacolone in 61% yield, as determined by comparison of the ^1H NMR spectrum to that of the initial solution. The sample was then opened and the solution was passed through a short column of silica to remove the ruthenium complex, eluting with 1 mL of ether. Gas chromatographic analysis of the eluent showed the presence of pinacolone, as determined by comparison of the retention time to that of an authentic sample and coinjection of the eluent and the authentic sample.

Reaction with Trimethylsilane. The third portion of 20, prepared as described in the reaction of 20 with H_2, was placed in an NMR tube, and to this tube was added 0.0121 mmol (1.0 equiv) of trimethylsilane by vacuum transfer. The sample was then heated to 85 °C for 2 h, after which time ^1H and $^{31}P\{^1H\}$ NMR spectroscopy showed formation of $(PMe_3)_3Ru(CH_2PMe_2)(H)$ in 40% yield and $Me_3SiOC(CH_2)CMe_3$ in 43% yield as determined by comparison to the initial solution described in the addition of H_2 to 20. The sample tube was then opened and the solution was passed through a short column of silica to remove the ruthenium complex, eluting with 1 mL of ether. Gas chromatographic analysis of the eluent showed the presence of $Me_3SiOC(CH_2)CMe_3$, as determined by comparison of the retention time

to an authentic sample, as well as coinjection of the eluent and a solution of the authentic sample.

X-ray Crystal Structure Determination of 17. (a) Isolation and Mounting. Crystals of the compound were obtained by slow crystallization from pentane at −40 °C. Fragments cleaved from some of these crystals were mounted in thin-wall capillaries in an inert atmosphere glovebox and then the capillaries were flame sealed.

The crystal used for data collection was then transferred to our Enraf-Nonius CAD-4 diffractometer and centered in the beam. It was cooled to −90 °C by a nitrogen flow low-temperature apparatus, which had been previously calibrated by a thermocouple placed at the sample position. Automatic peak search and indexing procedures yielded a monoclinic reduced primitive cell. Inspection of the Niggli values revealed no conventional cell or higher symmetry. The final cell parameters and specific data collection parameters for this data set are given in Table I.

(b) Structure Determination. The 3227 raw intensity data were converted to structure factor amplitudes and their esd's by correction for scan speed, background, and Lorentz and polarization effects. Inspection of the intensity standards revealed a reduction by 7% of the original intensity. The data were corrected for this decay. Inspection of the azimuthal scan data showed a variation $I_{min}/I_{max} = 0.94$ for the average curve. An empirical correction based on the observed variation was applied to the data. Inspection of the systematic absences indicated uniquely the space group $P2_1/n$. Removal of systematically absent and redundant data left 2890 unique data in the final data set.

The structure was solved by Patterson methods and refined via standard least-squares and Fourier techniques. Hydrogen atoms were assigned idealized locations and values of B_{iso} approximately 1.15 times the B_{eqv} of the atoms to which they were attached. They were included in structure factor calculations, but were not refined. The final residuals for 190 variables refined against the 2430 data for which $F_2 > 3\sigma(F^2)$ were $R = 3.89\%$, $R_w = 5.11\%$, and GOF = 2.23. The R value for all 2890 data was 5.60%.

The quantity minimized by the least-squares program was $\sum w(|F_o| - |F_c|)^2$, where w is the weight of a given observation. The p factor, used to reduce the weight of intense reflections, was set to 0.03 throughout the refinement. The analytical forms of the scattering factor tables for the neutral atoms were imaginary components of anomalous dispersion. Inspection of the residuals ordered in ranges of $\sin\theta/\lambda$, $|F_o|$, and parity and the values of the individual indexes showed no unusual features or trends. The largest peak in the final difference Fourier map had an electron density of 0.77 $e^-/Å^3$, and the lowest excursion was −0.69 $e^-/Å^3$. Both were located near the Ru atom. There was no indication of secondary extinction in the high-intensity low-angle data.

The positional and thermal parameters of the non-hydrogen atoms were provided as supplementary material with the preliminary report of this compound,[14] along with anisotropic thermal parameters and the positions and thermal parameters of the hydrogen atoms, as well as a listing of the values of F_o and F_c.

X-ray Crystal Structure Determination of 15. (a) Isolation and Mounting. Crystals of the compound were obtained by cooling slowly a pentane solution of 15 and were mounted in a viscous oil. X-ray data were collected as for 17; the final cell parameters and specific data collection parameters are given in Table I.

(b) Structure Determination. The 3675 raw intensity data were converted to structure factor amplitudes and their esd's by correction for scan speed, background, and Lorentz and polarization effects. An empirical absorption correction was applied to the data. Inspection of the systematic absences indicated space group *Pnma*. Removal of systematically absent and redundant data left 3542 unique data in the final data set.

The structure was solved by Patterson methods and refined via standard least-squares and Fourier techniques. The final residuals for 126 variables refined against the 2497 data for which $F_2 > 3\sigma(F^2)$ were $R = 6.3\%$, $R_w = 7.9\%$, and GOF = 2.85. The R value for all 3542 data was 9.4%.

The data were analyzed as described for compound 17 and are also provided as supplementary material.

X-ray Crystal Structure Determination of 18. (a) Isolation and Mounting. Crystals of the compound were obtained by sublimation of 18 in a sealed tube at 55 °C for 2 weeks and were mounted as described for 15. X-ray data were collected as for 17; the final cell parameters and specific data collection parameters are given in Table I.

(b) Structure Determination. The 1441 raw intensity data were converted to structure factor amplitudes and their esd's by correction for scan speed, background, and Lorentz and polarization effects. An empirical absorption correction was applied to the data. Inspection of the systematic absences indicated space group *Pnma*. Removal of systematically absent and redundant data left 1276 unique data in the final data set.

The structure was solved by Patterson methods and refined via standard least-squares and Fourier techniques. The final residuals for 51 variables refined against the 820 data for which $F_2 > 3\sigma(F^2)$ were $R = 7.8\%$, $R_w = 9.2\%$, and GOF = 3.07. The R value for all 2890 data was 12.5%.

The quantity minimized by the least-squares program was $\sum w(|F_o| - |F_c|)^2$, where w is the weight of a given observation. The p factor, used to reduce the weight of intense reflections, was set to 0.03 throughout the refinement. The data were analyzed as described for compound 17 and were provided as supplementary material with the preliminary report of this compound.[14]

Acknowledgment. We greatly appreciate support for this work from the National Institutes of Health (Grant GM-25459). Crystal structures were performed by Dr. Frederick J. Hollander at the University of California, Berkeley (CHEXRAY) facility.

Supplementary Material Available: Tables of positional parameters, anisotropic thermal parameters, root-mean-square amplitudes of anisotropic displacements, and least-squares planes for compound 15 (3 pages); a table of structure factors for compound 15 (21 pages).[44] This material is provided with the archival edition of the journal, available in many libraries; alternatively, ordering information is given on any current masthead page.

(44) Data for 17 and 18 were submitted with the previous report of these compounds.[14]